Earth-Science Reviews 262 (2025) 105063

Contents lists available at ScienceDirect

Earth-Science Reviews

journal homepage: www.elsevier.com/locate/earscirev

Invited Review

An overview of observed changes in precipitation totals and extremes over global land, with a focus on Africa

Tewodros Addisu Yate [a,b], Guoyu Ren [a,c,*]

[a] School of Environmental Studies, China University of Geosciences (CUG), Wuhan 430074, China
[b] Meteorology and Hydrology Faculty, Water Technology Institute, Arba Minch University, Arba Minch, Ethiopia
[c] Laboratory for Climate Studies, National Climate Center, China Meteorological Administration, Beijing 100081, China

ARTICLE INFO

Keywords:
Precipitation total
Extremes
Trend
Significance
In situ data
Station coverage
Accessibility

ABSTRACT

Precipitation is one of the crucial climatic variables that has significant impact on the natural and human systems, with several important sectors of the Earth's system responding to its spatiotemporal variability. Consequently, various studies are conducted on global and regional scales to evaluate changes and trends in precipitation, with more emphasis on extremes. This review assesses existing studies on precipitation trends conducted using *in situ* data or gauge-based datasets, examining their comparability and consistency to identify regional trends. It also seeks to demonstrate the pressing challenges related to the availability and accessibility of precipitation data, with a particular focus on Africa. The existing gauge-based global and regional studies are limited and generally diverse, making it difficult to infer robust regional trends from their findings. Complex differences are observed in data periods, analysis region, methods, precipitation metrics, and the type of datasets used. This review notes that there is uneven station distribution in each continent, and that this is also mirrored in the existing global datasets, while Africa constitutes one of the least covered global regions. Yet, a few studies agree that long-term precipitation totals exhibit non-significant decreasing trends over northern Africa and significantly decreasing trends in parts of western Africa. Conversely, long-term annual precipitation totals have increased significantly over Asia, northern and central Europe, southern Canada and the eastern United States. Generally, despite accounting for different analysis periods, total and extreme trends match up for most global regions. Areas with significant increasing extreme trends, such as RX1day, RX5day and R95pTOT indices, include South Africa, eastern Asia, Canada, northern and central Europe, northeastern United States, and western Australia. Overall, more efforts are needed to significantly expand station coverage across Africa and ease restrictions to allow greater access to data. Initiatives to establish and monitor climate stations across Africa need to be supported. Regional studies that use *in situ* or gauge-based datasets need to increase and employ comparable analysis regions and data periods, as well as assess and adjust for systematic biases in precipitation data at urban stations.

1. Introduction

Precipitation is a fundamental component of the hydrological cycle, governing water resources availability for life on Earth and ecosystems, and maintaining global water balance by redistributing water across the planet (Zhan et al., 2018; Carvalho, 2020). Several sectors including water, agriculture, energy, industry, and infrastructure are impacted by precipitation, particularly the extremes (Zhan et al., 2018; Contractor et al., 2021; IPCC, 2022; Palmer et al., 2023). Droughts and floods, in particular, have caused significant damage to social, economic, and environmental systems (Haile et al., 2019; Sugg et al., 2020; Merz et al., 2021; Lieber et al., 2022; IPCC, 2022; Coly et al., 2023; Palmer et al., 2023; Adeel et al., 2023). As a result, various studies have been conducted on global and regional scales to evaluate precipitation changes, with more focus being placed on trends in precipitation extremes.

While the observed global and regional warming trend is well-established, changes in precipitation exhibit complex spatiotemporal heterogeneity across various regions (e.g. Choi et al., 2009; O'gorman, 2015; Easterling et al., 2017; Giorgi et al., 2019; Carvalho, 2020; Contractor et al., 2021; Mcbride et al., 2022; Ren et al., 2023; Mckay et al., 2023). Changes in the total and extreme precipitation, along with variations in their frequency and intensity, have become more evident in

* Corresponding author at: School of Environmental Studies, China University of Geosciences (CUG), Wuhan 430074, China.
E-mail address: guoyoo@cma.gov.cn (G. Ren).

https://doi.org/10.1016/j.earscirev.2025.105063
Received 6 February 2024; Received in revised form 3 December 2024; Accepted 2 February 2025
Available online 8 February 2025

a few large regions of the northern hemisphere, with the warming climate assumed to have played a role (Alexander et al., 2007; O'gorman, 2015; Ren et al., 2017; Easterling et al., 2017; Feng et al., 2019; Myhre et al., 2019; Papalexiou and Montanari, 2019; Ren et al., 2021; IPCC, 2021; Kuttippurath et al., 2021; Wang et al., 2023). Moreover, changes in the overall precipitation distribution and the ratio of snowfall to precipitation have been observed (Zhang et al., 2000; Vincent et al., 2018; Feng et al., 2019; Contractor et al., 2021; Harp and Horton, 2022; Tolhurst et al., 2023; Wang et al., 2023; Suriano et al., 2023).

Theoretical analysis and climate model simulations suggest that an anthropogenic increase in global surface temperature leads to a rise in global average precipitation (Feng et al., 2019; Myhre et al., 2019; Liu et al., 2022). Increasing surface temperature can change atmospheric moisture content as per the Clausius–Clapeyron relation, which indicates an around 7 % increase in atmospheric water holding capacity for each degree of warming (Giorgi et al., 2019; Mcbride et al., 2022). However, the magnitude of this increase varies among different gauge-based global datasets and across spatial scales (Nguyen et al., 2018; Feng et al., 2019; Harp and Horton, 2022).

Despite reports of a global scale increase in maximum one-day precipitation that is consistent with the Clausius–Clapeyron relation (IPCC, 2021), the effect of surface warming on the spatiotemporal patterns of regional precipitation is influenced by other factors and multi-decadal natural variability (Moustakis et al., 2020; Contractor et al., 2021; Ren et al., 2021; Harp and Horton, 2022). Long-term precipitation change in a region can be driven by dynamical mechanisms and local forcing (Carvalho, 2020; IPCC, 2021; Madakumbura et al., 2021; Harp and Horton, 2022; Palmer et al., 2023; Mckay et al., 2023), in addition to the thermodynamic forcing due to the Clausius–Clapeyron relation (Alizadeh and Babaei, 2022). Moreover, changes in station coverage over time can influence the consistency of regional long-term trends, as shown by Ren et al. (2017), and require consideration.

Regional studies are capable of detailing the spatiotemporal changes in precipitation with greater precision, effectively highlighting local patterns. It is important to note that global scale generalization of changes in precipitation may be deceptive, as different regions can exhibit diverse trends and inconsistent spatial patterns. This underlines the importance of examining regional studies and assessing their comparability to understand local trends accurately. However, as this review intends to illustrate, comparing regional studies to evaluate regional trends in precipitation is often difficult. Therefore, it is necessary to show the existing differentiation and the depth of the challenge it has posed.

Lack of long-term *in situ* data is the major factor significantly hampering comprehensive analyses of precipitation trends (Sun et al., 2017; Zhan et al., 2018; Dey et al., 2019; Contractor et al., 2021; Ren et al., 2023). According to IPCC, only a few regions of the earth have *in situ* records that extend prior to 1950, and this has led to discrepancies in the findings of studies analyzing long-term global trends of precipitation anomalies (IPCC, 2021). Besides the challenge of data longevity, many meteorological stations face significant issues such as missing records, poor data quality, and inhomogeneity, with these problems being particularly severe in developing nations (Omondi et al., 2014; Dezfuli et al., 2017; Muthoni et al., 2019; Carvalho, 2020; Contractor et al., 2021; Ren et al., 2023; Wang et al., 2023). Although the number of stations available to precipitation datasets has shown an overall increase over time, there has been a recent decline. This decline has been related, among other factors, to the change in data policy from the suppliers (Funk et al., 2015a; Sun et al., 2017; Dinku, 2019; Contractor et al., 2020; Carvalho, 2020; Bliefernicht et al., 2021; IPCC, 2022).

In this review, studies conducted based on *in situ* data or gauge-based gridded datasets are reviewed to comprehend trends in precipitation totals (beginning in 1901 or before) and extremes (beginning in 1981 or before) over various regions, with a particular emphasis on Africa. It seeks to assess the breadth of availability of such studies, their comparability, the challenges they face and the progress made. The in-depth data issues pertaining to the African continent are illustrated to emphasize the pressing need for improved coverage and accessibility. Due to the limitations and uncertainties associated with reanalysis data and climate models (Choi et al., 2009; Zhang et al., 2011; Zhan et al., 2018; Le Coz and Van De Giesen, 2020; Contractor et al., 2020; Dosio et al., 2021), and also word limit of the paper, studies that rely partly or entirely on reanalysis and simulations are excluded, or only findings based on observational data are included.

Satellite precipitation data, while extensive and valuable for global coverage, often exhibit considerable disparities when compared to *in situ* measurements (Sun et al., 2017; Alexander et al., 2019; Harrison et al., 2019; Le Coz and Van De Giesen, 2020; Alexander et al., 2020; Kagone et al., 2023). In regions where station networks are sparse, such as Africa, satellite data can be helpful in providing precipitation estimates. However, they are still far from matching the precision of *in situ* measurements of precipitation, particularly on a daily scale. The accuracy of satellite-based precipitation estimates considerably varies depending on precipitation type, intensity, season, and topography (Stampoulis et al., 2013; Maggioni et al., 2016; Chen et al., 2021; Afzali Gorooh et al., 2023). The use of different measurement techniques and algorithms lead to heterogeneous precipitation estimates among satellites across different regions and time periods (Sun et al., 2017; Le Coz and Van De Giesen, 2020). Furthermore, the short temporal span of satellite records further limits their use for long-term assessments, such as centennial trends (Sun et al., 2017; Contractor et al., 2021). For this reason, studies that have used satellite products are also excluded from this review.

Studies employ diverse gauge-based datasets, in addition to various methods, to address data limitations, which can occasionally affect the analysis results. In view of this, Table 1 provides an overview of gauge-based global datasets that are used in the studies reviewed in this article, including those referenced in IPCC (2021). Table 1 includes only the most recent versions of the datasets, which typically provide details or references to older versions, if available. Since this review concentrates on Africa, various regions of the continent are referenced, and a map of the continent is provided in Fig. 1 to help identify the locations of each country. For consistency, the term 'precipitation' is used throughout this review, although 'rainfall' may be more suitable for precipitation regimes in low-latitude regions, such as tropical zones of Africa and South America.

2. Long-term trends in precipitation total

Summarized based on the results of the gauge-based global and regional studies assessed in this section, which employ a data period of nearly a century (>70 years), Fig. 2 highlights areas with significant long-term annual precipitation trends. Most of these studies have a data period that starts around 1901, and therefore capture trends throughout the last century. Nonetheless, there are differences in the end dates of the data periods, with some extending to recent years, such as 2019 and 2020. The summary of the regional studies is presented in Table 2 and Appendix A. In the Northern Hemisphere, mid- to high-latitude regions see an increase in annual total precipitation, while tropical and subtropical areas undergo a decrease. It should be noted that the gauge-based global studies—which are also well used in this review—are not shown in Table 2 and Appendix A.

2.1. Africa

The long-term precipitation trend over Africa is among the least understood and poorly described due in large part to the limited station coverage across the continent. Existing gauge-based studies have focused on analyzing recent changes in precipitation total, spanning short periods of time, and on assessing the factors driving precipitation variability (e.g. Omondi et al., 2012; Omondi et al., 2013; Liebmann et al., 2014; Maidment et al., 2015; Muthoni et al., 2019; Lüdecke et al., 2021; Hoell et al., 2021; Palmer et al., 2023). Precipitation changes over

Table 1
Details of the global datasets used in the studies that are assessed in this review.

Dataset	Developed and/or hosted by	Frequency	Period	Coverage	Grid size	Reference
CGP1.0	China Meteorological Administration (CMA)	Monthly	1901–2013	Global land	5° × 5°	Yang et al. (2016)
GHCN-D	National Oceanic and Atmospheric Administration/National Centers for Environmental Information (NOAA/NCEI)	Daily	1951–2023	Global land	–	Menne et al. (2012)
CPC-Global	National Oceanic and Atmospheric Administration/Climate Prediction Center (NOAA/CPC)	Daily	1979–2023	Global land	0.5° × 0.5°	Chen et al. (2008); Xie et al. (2010)
CRU TS version 4.04	The Climate Research Unit (CRU), University of East Anglia	Monthly	1901–2019	Global land	0.5° × 0.5°	Harris et al. (2020)
version 4.0			1901–2015			Harris et al. (2020)
earlier version			1901–2014			Harris et al. (2014)
GPCC–FDD v2022	Global Precipitation Climatology Centre at Deutscher Wetterdienst (DWD)	Daily	1982–2020	Global land	1° × 1°	Ziese et al. (2022)
GPCC–FDM v2022		Monthly	1891–2020		0.25°, 0.5°, 1°, 2.5°	Schneider et al. (2022a); Schneider et al. (2022b)
UDEL–TS v4.01	Center for Climatic Research, University of Delaware	Monthly	1900–2017	Global land	0.5° × 0.5°	Matsuura and Willmott (2018)
REGEN_ALL_2019	ARC Centre of Excellence for Climate System Science (ARCCSS), University of New South Wales	Daily	1950–2016	Global land	1° × 1°	Contractor et al. (2020)

Fig. 1. Map of Africa highlighting the locations of each country.

northern Africa have relatively more references because studies across the Mediterranean and Arab regions have included this region (Philandras et al., 2011; Donat et al., 2014; Caloiero et al., 2018; Zittis, 2018). Liebmann et al. (2014) and Muthoni et al. (2019) analyze precipitation trends in the eastern Africa region, but their studies are limited to relatively short data periods: 1979–2012 and 1981–2017, respectively.

Onyutha (2018) finds a mix of annual precipitation trends across Africa during the period 1901–2015. Northern Africa primarily exhibits non-significant trends, while significant trends are evident in scattered pockets of sub-Saharan Africa (Fig. 3–a) (Onyutha, 2018). Zittis (2018) also shows overall decreasing precipitation trends over northern Africa for the period 1901–2014, as do Caloiero et al. (2018) for large parts of northern Africa, specifically along the coastal regions of Morocco,

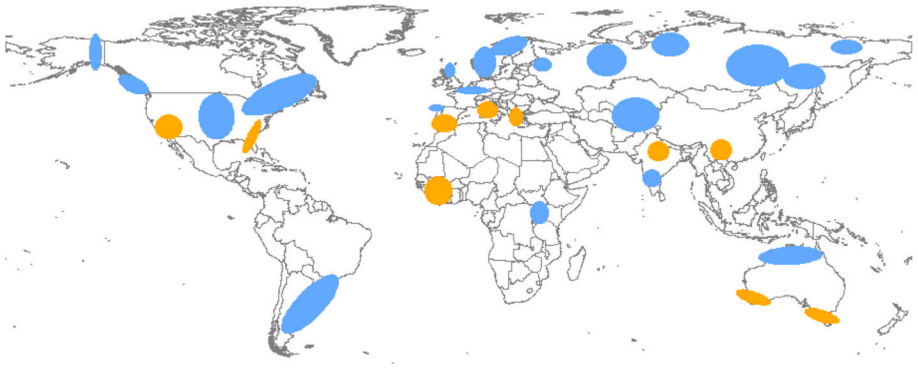

Fig. 2. Approximate areas demonstrating significant annual precipitation total trends (at the 5 %) as evidenced by at least two studies for each region that use nearly centennial data period. Areas with significant increasing and decreasing trends are shown with blue and yellow shaded polygons, respectively. The size of the polygons increases with the number of neighboring stations or grids with agreement. (For interpretation of the references to colour in this figure legend, the reader is referred to the web version of this article.)

Table 2
Summary of the gauge-based studies on long-term precipitation trends over African regions and key findings.

Study	Spatial coverage	Dataset	Data Period	Precipitation metrics	Method	Areas showing significant trend (at $P < 0.05$)	
					Trend slope and significance	Significantly increasing trend	Significantly decreasing trend
Onyutha (2018)	Africa	CRU v. 4.0	1901–2015	annual precipitation (mm/year)	CSD method by Onyutha (2016b)	Eastern and periphery of western equatorial Africa; northern Madagascar.	Section of western Africa such as Senegal, southern Mali, Guinea, Sierra Leone and Liberia.
Tierney et al. (2015)	eastern Africa (20°N–5°S & 30°E–55°E)	GPCC v.6.0	1901–2010	mean annual precipitation (%/year)	Man-Kendal (Mann, 1945, Kendall, 1962)	For the September–November season: southern Kenya and Lake Victoria	Eastern Sudan along the Nile River, southeast Ethiopia; broadening to encompass south Somalia and Kenya for June–August season
Zittis (2018)	Mediterranean, Middle East, northern Africa and broad areas of Ethiopia	CRU v. 3.24.0; UDEL v.4.01; GPCC v.6.0	1901–2014	mean annual precipitation (mm/decade)	linear regression model, F-statistic	–	Northern Africa in GPCC and UDEL datasets; Sahel region in CRU and GPCC datasets; Ethiopian highlands in GPCC dataset.
Caloiero et al. (2018)	Europe and Mediterranean	GPCC v.6.0	1901–2009	annual precipitation (mm/decade)	Theil–Sen estimator (Sen, 1968); Man-Kendal (Mann, 1945, Kendall, 1962)	in the vicinity of Tunis	coastal regions of Morocco, Algeria and Libya.
Philandras et al. (2011)	Mediterranean	CRU version TS 3.1	1901–2009	annual total precipitation (mm/year)	Man-Kendal (Mann, 1945, Kendall, 1962)	in the vicinity of northern Tunisia (non- significant)	northern parts of Morocco and central northern coastal regions of Algeria.

Study	Spatial coverage	Dataset	Data Period	Precipitation metrics	Method	Areas showing significant trend (at $P < 0.01$)	
					Trend slope and significance	Significantly increasing	Significantly decreasing
Nicholson et al. (2018)	African regions	station data	≈1850–2014	standardized departure	Man-Kendal (Mann, 1945, Kendall, 1962)	Gabon, Congo: 1877–2014;	coastal Algeria and coastal Tunisia: 1838–2014; Sahel: 1853–2014; Cameroon: 1889–2014;

Algeria, and Libya during 1901–2009. Philandras et al. (2011) find a similar result for northern Africa (above 30° N) over the same period. Nicholson et al. (2018) find decreasing annual precipitation trends in the coastal areas of northern African countries, and the Sahel region from the mid-19th century to 2014, while noting non-significant annual trends in southern Africa. In western Africa, significant decreasing trends are seen in areas near Senegal, southern Mali, Guinea, Sierra Leone and Liberia (Fig. 3–a and Fig. 4–a) (Onyutha, 2018). Contractor et al. (2021) also find decreasing annual precipitation trends over western Africa for a shorter data period, 1950–2016. Fig. 1 illustrates significant decreases in this region of western Africa.

On the other hand, a significant increasing trend is evident along the coastal regions of western equatorial Africa, including Gabon and the southwestern parts of the Republic of Congo, as well as over the eastern equatorial Africa surroundings, such as northeastern Democratic Republic of Congo, Rwanda, Burundi, Lake Victoria, and the northern half of Madagascar (Fig. 3–a and Fig. 4–a) (Onyutha, 2018). Tierney et al. (2015) demonstrate a predominantly decreasing trend in annual mean precipitation over the Eastern Africa region (20°N–5°S & 30°E–55°E) during 1901–2010. The spatial pattern of the annual precipitation trends shown by Onyutha (2018) for the period 1901–2015 closely correspond with an earlier study by Hulme et al. (2001), which covers a shorter data

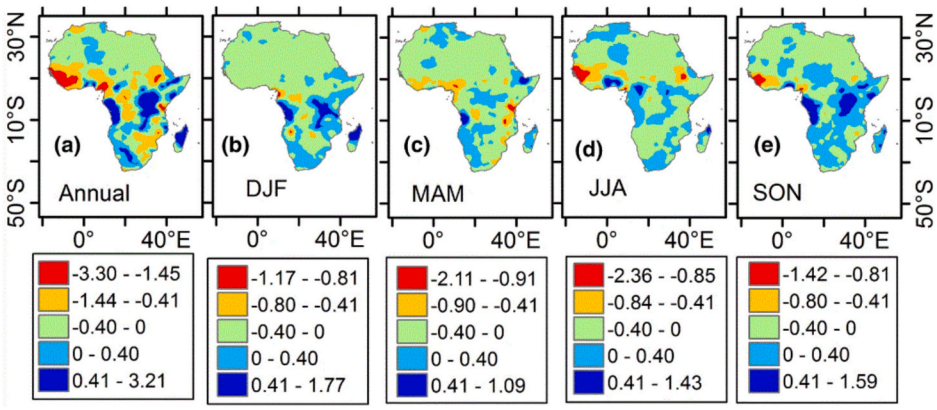

Fig. 3. Spatial patterns of the linear trend in precipitation total across Africa over the period 1901–2015 (from Onyutha (2018)). Positive values indicate increasing trends, while negative values indicate decreasing trends. DJF, MAM, JJA and SON designate December to February, March to May, June to August, and September to November seasons, respectively.

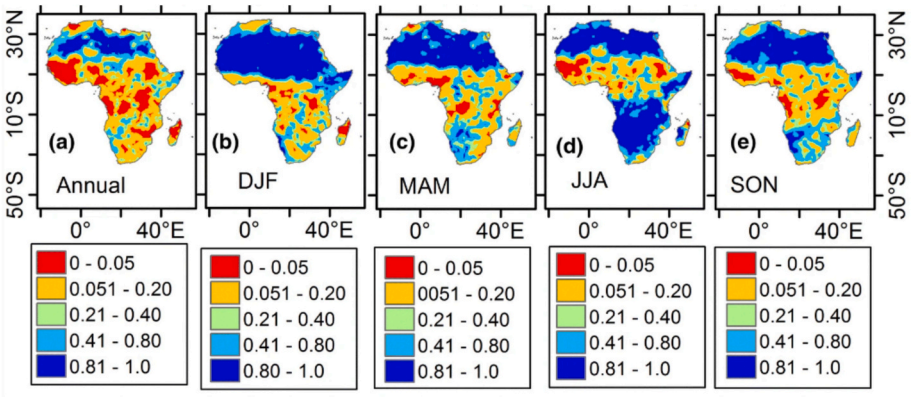

Fig. 4. Spatial map depicting the significance of the precipitation trend over the period 1901–2015 (from Onyutha (2018)). As indicated by the *p*-values in the legend, the red-highlighted areas on the map ($p<0.05$) represent regions with significant trends. DJF, MAM, JJA, and SON designate the December to February, March to May, June to August, and September to November seasons, respectively. (For interpretation of the references to colour in this figure legend, the reader is referred to the web version of this article.)

period, 1901–1995.

The precipitation trend for the winter season (December to February) is found to be non-significant for large parts of Africa, except for small equatorial regions like Lake Victoria and northern half of Madagascar, where increases are significant (Onyutha, 2018; Lim Kam Sian et al., 2021). Similarly, for the spring season (March to May), most of the continent shows non-significant trends, except for areas such as southern Nigeria, western Cameroon, and northeastern Tanzania, where there are significant increases. A significant decreasing trend is evident in western Africa over Senegal and southern Mali during summer (June to August), highlighting this season's substantial impact on the annual precipitation trend in that region (Onyutha, 2018). Tierney et al. (2015) find a significant decrease during the June to August season over eastern Sudan along the Nile River, southeast Ethiopia, southern Somalia, and Kenya. For autumn (September to November), Onyutha (2018) find a significant increase in precipitation over western equatorial Africa around Gabon and the southern part of the Republic of Congo, as well as over Lake Victoria in eastern equatorial Africa. Similarly, Tierney et al. (2015) find a significant increasing trend for this season over southern Kenya and Lake Victoria.

The IPCC (2021) indicates a considerable decrease in annual precipitation across tropical western Africa and equatorial Africa during the period 1901–2019. This does not fully align with the findings by Onyutha (2018), which show largely increasing trends across equatorial Africa, particularly south of the equator. The inconsistency can be due to differences in data periods and methodologies. A new methodology (Onyutha, 2016) is employed by Onyutha (2018). Applying established methodologies would be more suitable for regions with sparse station networks, like most of Africa, and facilitates result comparisons among studies. Due to the limited number of stations in the CRU dataset representing sub-Saharan Africa, Onyutha (2018) cautions that results should be interpreted carefully. Similarly, Contractor et al. (2021) attribute significant uncertainty to their findings for African regions due to inadequate data.

Variations in trend significance can be observed across different global datasets in regions with sparse station coverage (Zittis, 2018). At least one of the three datasets used by Zittis (2018) (Table 2) shows a considerable discrepancy in annual precipitation amounts compared to the others, except in the Iberian and Balkans regions. In these regions, there is good agreement among the three datasets regarding both the amount and temporal pattern, attributed to the presence of dense station networks (Zittis, 2018). The quality of trend analysis is also determined by the application of appropriate precipitation representation. Ren et al. (2023) recommend using precipitation anomaly percentage for analyzing precipitation total trends, as it accounts for local precipitation climates and more clearly depicts patterns on a broad scale.

Similarly, the methods used in the analysis also affect the results. It is suggested to use a combination of the Theil–Sen estimator (Sen, 1968) and the Mann-Kendall (MK) test (Mann, 1945; Kendall, 1962) to compute the slope of the trend and assess statistical significance, respectively (Caloiero et al., 2018; Yang et al., 2019; Contractor et al., 2021; Ren et al., 2023). As the application of the Mann-Kendall test

requires the data to be free from serial correlation, an evaluation of autocorrelation is necessary beforehand (Ren et al., 2023). If significant serial correlation is detected, a procedure called trend-free pre-whitening (TFPW) can be applied to eliminate the autocorrelation (Yue et al., 2002). More conveniently, to overcome this requirement, a modified version of the Mann-Kendall (MK) test can be applied (Zhang et al., 2000; Contractor et al., 2021; Yu et al., 2022). Gauge-based studies on long-term precipitation trends involving African regions are summarized in Table 2, along with their key findings.

2.2. Other regions

Asia. Over the past decade, a research group connecting the China University of Geosciences (Wuhan) and the China Meteorological Administration (CMA) has been working on developing datasets, improving methods, and conducting studies related to Asia and its subregions (such as Ren and Zhou, 2014, Ren et al., 2015, Yang et al., 2016, Ren et al., 2017, Zhan et al., 2017, Zhan et al., 2018, Zhan et al., 2019, Zhan et al., 2022). Building on this, Ren et al. (2023) recently provide an updated dataset, and comprehensively assess changes in temperature and precipitation over the Asian continent during the periods 1901–2020 and 1901–2019, respectively.

The findings by Ren et al. (2023) show significant increase in precipitation over Asia during the period 1901–2019, as previously shown by Zhan et al. (2018) for the period 1901–2016. According to the time series illustrated by Ren et al. (2023), the continent sees persistent dry spells on average from 1900 to 1950, while positive anomalies remain dominant during the second half of the 20th century. Increases over the recent period (2001–2019) have larger magnitudes than the long-term trends (Ren et al., 2023). Spatially, increases are more pronounced along the high-latitude regions of the continent, and along mid-latitudes between 60° E and 80° E longitudes, as illustrated in Fig. 2. The precipitation trend over mainland China has generally remained stable during 1901–2019 (Ren et al., 2023), as illustrated for eastern China by Zhan and Ren (2023). However, since 1960, Ren et al. (2023) find increasing trends over China, particularly over the western half, as previously shown by Zhai et al. (2005) for the period 1951–2000. Zhang et al. (2020), after adjusting for biases resulting from systematic errors (Zhang et al., 2019), provide further detail on the regional patterns, and illustrate increasing trends across northwest, agreeing with Ren et al. (2016), and southeast China.

The IPCC (2021) indication of a significant decreasing trend in annual precipitation over South Asia is not fully evidenced in the results of Ren et al. (2023) and Zhan et al. (2018). Instead, their findings show that a larger proportion of the grids exhibit non-significant trends across South Asia, with a few significant increasing trends evident over northern India and significant decreasing trends over southern India, as shown in Fig. 2 (Ren et al., 2023). The difference with IPCC (2021) could be due to the different study periods, datasets used or precipitation metrics applied. The findings by Ren et al. (2023) and Zhan et al. (2018) regarding the long-term precipitation trend over South Asia align with those of Kumar et al. (2010), Mondal et al. (2015) and Ren et al. (2017), despite their use of different data periods. The substantial long-term precipitation increase over North Asia reported by Ren et al. (2023) and Zhan et al. (2018) is well consistent with the IPCC's assessment over northern Eurasia (IPCC, 2021), as shown in Fig. 2. While the overall long-term trend over East Asia is found to be non-significant, small-scale studies (such as Duan et al., 2015) can reveal significant local trends.

Europe. Assessing changes in precipitation at sub-continental scales has received more attention than at continental scales in Europe. Vicente-Serrano et al. (2020) find non-significant trends in regional average annual and seasonal precipitation over southwest Europe during 1870–2018, with significant trends limited to short periods. For instance, Peña-Angulo et al. (2020) demonstrate significant decreasing trend from 1960 to 2000 during the winter season. Over the period 1901–2009, Caloiero et al. (2018) find significant decreasing trend in annual precipitation across the southern European region—Italy, southern Austria, southern Spain, Albania and Greece, as well as in Northern Ireland and the northern areas of Norway. Supporting these findings, Philandras et al. (2011) show considerable decreasing trend in annual precipitation along the coastal areas of southern Europe, including central and northern Italy, Croatia, and southern Spain during the same period. While Caporali et al. (2021) report similar findings regarding Italy, Hadi and Tombul (2018) find a generally decreasing trend across Turkey during 1901–2014. Conversely, there have been significant increasing trends across the western and northern European regions, including Norway, Sweden, Germany, France, north-western Russia, northern United Kingdom, Netherlands and Estonia (Caloiero et al., 2018). Overall, while annual precipitation has largely increased in western and northern Europe over the past century, it has generally dropped in southern Europe, as illustrated in Fig. 2.

North America. Annual precipitation averaged over the United States has increased over the past century and recent decades (Easterling et al., 2017; EPA, 2022). According to Karl and Knight (1998), the increasing trend in precipitation across the United States during the 20th century (1910–1996) is largely due to a rise in extreme precipitation events. Supporting this, Easterling et al. (2017) report strong positive trends in extreme precipitation events over a large part of the country during 1901–2015. From a regional perspective, as depicted in Fig. 2, increasing trends are found over the eastern United States, particularly in the Northeast and Midwest regions, while decreasing trends are evident over the western United States, particularly in the Southwest region (Easterling et al., 2017; IPCC, 2021; EPA, 2022; Harp and Horton, 2022). Over a shorter data period from 1950 to 2016, Contractor et al. (2021) find a positive but non-significant trend averaged across the country, with the eastern United States exhibiting increasing annual precipitation trends.

Due to insufficient data for northern Canada before 1950, studies limit their centennial analysis to southern Canada (below 60° N) or most of their stations originate from this region. As previously shown by Zhang et al. (2000) for 1900–1998 and by Vincent et al. (2018) for 1900–2012, Wang et al. (2023) also illustrate an increasing trend in annual precipitation over southern Canada during 1900–2019, with significant trends found in the eastern and western coastal areas, as shown in Fig. 2. Similarly, Wang et al. (2023) find increasing trend over Canada during 1948–2012, a finding supported by Contractor et al. (2021) during 1950–2016, with significant trends being evident along the east and west coasts of the country.

Moreover, Zhang et al. (2000) find increases in the annual ratio of snowfall to precipitation over southern Canada during 1900–1998, with an increase in precipitation during winter—a season typically associated with snowfall—being suggested as the cause. Similarly, Vincent et al. (2018) find an increasing trend in the number of days with snowfall over southern Canada during 1900–2012. However, they also indicate a decreasing trend in the number of days with snowfall from the mid-1970s to 2012. Regarding changes in snowfall under the warming climate, studies exhibit diverse results across different global regions and seasons (Davis et al., 1999; O'gorman, 2014; Danco et al., 2016; Deng et al., 2017; Easterling et al., 2017; Zhou et al., 2018; Harp and Horton, 2022; Nicola et al., 2023).

South America. South America is one of the global regions where the scarcity of observational data has hindered progress in studying long-term precipitation changes. Most of the existing studies is based on short data periods or has limited spatial coverage (Haylock et al., 2006; Aravena and Luckman, 2009; De Los Milagros Skansi et al., 2013; De Barros Soares et al., 2017; Almeida et al., 2017; Haghtalab et al., 2020). Other small-scale studies (not shown here) that are not available in English also exist. A significant upward trend in precipitation over the southeastern region of South America is illustrated by Varuolo-Clarke et al. (2021) over 1901–2016 and by Contractor et al. (2021) over 1950–2016, as shown in Fig. 2. Increasing trends across a comparable region of the continent are previously reported by Haylock et al. (2006)

and De Los Milagros Skansi et al. (2013) during 1960–2000 and 1950–2010, respectively. In contrast, decreasing trends are shown over southern Peru and southern Chile (Haylock et al., 2006).

Australia. It is important to highlight that the central region of Australia, extending southward, has limited station coverage. Dey et al. (2019) demonstrate an increasing trend in annual precipitation over large parts of Australia during 1910–2015, with significant increases observed in the northern areas. This finding is corroborated by He et al. (2022), who also report a significantly increasing trend in the northern region during 1910–2017. The trend is stronger and more apparent for the recent decades, 1986–2015 (Dey et al., 2019). For a longer period of 1901–2019, the IPCC (2021) reports a significant increasing trend in annual precipitation over a comparable region of the continent. Contractor et al. (2018) show considerable increases in annual precipitation over northwest Australia during 1950–2016, a trend that Dai (2021) confirms for the period 1950–2018. Comparing the two periods of 1958–1985 and 1986–2013, Contractor et al. (2018) also illustrate an increase in the number of wet days in northern Australia. Conversely, Dey et al. (2019) find a decreasing trend in precipitation over southwest and southeast Australia during 1910–2015, which Contractor et al. (2018) also note during 1950–2016. Mckay et al. (2023) further analyze and review this drying trend that is evident in southwest and southeast Australia.

3. Indices for extreme precipitation analysis

Extremes are responsible for most observed impacts and damages (WMO, 2009; Choi et al., 2009; Zhang et al., 2011; Zhan et al., 2017; Dunn et al., 2020; Ren et al., 2021; Contractor et al., 2021). It is therefore more pertinent to characterize the tail of the precipitation distribution (Zhang et al., 2011). Nevertheless, to analyze precipitation extremes, daily or sub-daily precipitation data—which are less available than monthly records—are required (WMO, 2009; Zhang et al., 2011; Zhan et al., 2017; Alexander et al., 2019; Dunn et al., 2020; Contractor et al., 2021). The limited availability is compounded by accessibility constraints related to the willingness and ability of countries to share the data (Alexander et al., 2006; Zhang et al., 2011; Donat et al., 2013b; Alexander et al., 2019; Dunn et al., 2020; Contractor et al., 2021). In order to overcome this restriction, it has become necessary to gather records in the form of derived metrics of extremes—extreme indices—which national meteorological organizations are more willing to provide (Zhang et al., 2011; Donat et al., 2013b; Alexander et al., 2019; Contractor et al., 2021). Furthermore, the availability of globally recognized indices for extreme analysis facilitates inter-comparison across regional studies and hence global-scale presentations (Zhang et al., 2011; Alexander et al., 2019; Dunn et al., 2020; Contractor et al., 2021).

In light of this, the Expert Team on Climate Change Detection and Indices (hereafter referred to as ETCCDI) defined a suite of globally recognized indices for temperature and precipitation extremes (Zhang et al., 2011; Alexander et al., 2019; Contractor et al., 2021). These indices have been pivotal in fostering regional collaborations and advancing studies focused on climate extremes over recent decades (Alexander et al., 2006; Choi et al., 2009; Zhang et al., 2011; Alexander, 2016; Alexander et al., 2019; Dunn et al., 2020). The ETCCDI indices are particularly effective in identifying moderate extremes that typically occur at least once a year (WMO, 2009; Zhang et al., 2011; Alexander, 2016; Dunn et al., 2020). To study more significant extremes that occur over longer time intervals, statistical methods developed from extreme value theory are employed (IPCC, 2021; Mcbride et al., 2022). Indices have also been developed to meet various goals and sector-specific needs (Alexander and Herold, 2016; Zhang et al., 2011; Donat et al., 2013b; Zhan et al., 2017; Alexander et al., 2019). Furthermore, new indices are being proposed to monitor extremes that require precipitation analyses at sub-daily scales (Lewis et al., 2019; Alexander et al., 2019).

As precipitation is the focus of this review, the precipitation-based ETCCDI indices are detailed in Table 3. As each indices track various aspects of extremes, it is recommended to use multiple categories of indices for a comprehensive analysis of extremes (Xiao-Juan et al., 2023). While most indices are typically calculated on an annual basis, the RX1day and RX5day indices are evaluated monthly (Zhan et al., 2017; Alexander et al., 2019; Alexander et al., 2020). To calculate the R95p and R99p indices, the 95th and 99th percentiles must be determined from the precipitation series of wet days during a climatological base period (Alexander et al., 2006; Choi et al., 2009; Zhang et al., 2011; Alexander et al., 2019). As per the recommendation of WMO, the period 1961–1990 has consistently been used as the climatological base period (Zhang et al., 2011). However, adjustments to this base period are sometimes inevitable to deal with data issues, as demonstrated by Omondi et al. (2014). It is important to ensure that any adjustments to the base period due to local data availability do not compromise the consistency needed for long-term climatic references and continuity with previous analyses. It may be necessary to modify thresholds of the indices, such as R10 and R20, to account for regional climate variations (Alexander et al., 2006; Alexander et al., 2007; Dunn et al., 2020).

It is crucial to underline the necessity of studying precipitation changes by breaking them down into frequency and intensity components. This differentiation is important not only because frequency and intensity have distinct impacts, but also because it helps in understanding how changes in frequency and intensity contribute to observed precipitation changes, as well as the relationship between these two components in a region (Contractor et al., 2018; Contractor et al., 2021). To fully assess changes in extreme precipitation, it is essential to consider the effects of changes in both the intensity and frequency of these extremes (Myhre et al., 2019). While the ETCCDI indices capture certain aspects of precipitation extremes, such as frequency (R1mm, R10mm, R20mm), intensity (SDII, RX1day, RX5day), and duration (CWD, CDD), they do not offer a comprehensive view of the entire precipitation distribution (Alexander et al., 2019; Contractor et al., 2021).

This indicates that ETCCDI indices should be complemented with analyses that cover the entire precipitation distribution for a more thorough insight on precipitation changes. Examining shifts in the full distribution of precipitation helps capture changes across the full spectrum of precipitation, which may not be evident when only considering mean or extreme values (Li and Yu, 2014; Contractor et al., 2018;

Table 3
Indices defined by the ETCCDI for precipitation extreme analysis (Zhang et al., 2011; Alexander et al., 2020). The R1mm index is based on the Rnnmm definition suggested by the ETCCDI, where 'nn' represents a user-defined threshold.

ID	Indicator Name	Indicator Definitions	Units
RX1day	Max 1–day precipitation amount	Monthly maximum 1–day precipitation	mm
RX5day	Max 5–day precipitation amount	Monthly maximum consecutive 5–day precipitation	mm
SDII	Simple daily intensity index	The ratio of annual total precipitation to the number of wet days (≥ 1 mm)	mm/day
R1mm	Number of wet days	Annual count when precipitation ≥1 mm	days
R10mm	Number of heavy precipitation days	Annual count when precipitation ≥10 mm	days
R20mm	Number of very heavy precipitation days	Annual count when precipitation ≥20 mm	days
CDD	Consecutive dry days	Maximum number of consecutive days when precipitation <1 mm	days
CWD	Consecutive wet days	Maximum number of consecutive days when precipitation ≥1 mm	days
R95p	Very wet days	Annual total precipitation from days >95th percentile	mm
R99p	Extremely wet days	Annual total precipitation from days >99th percentile	mm
PRCPTOT	Annual total wet-day precipitation	Annual total precipitation from days ≥1 mm	mm

Contractor et al., 2021; Tolhurst et al., 2023). It is documented that while extreme precipitation events may change, there can also be simultaneous changes in the frequency and intensity of light precipitation at the lower end of precipitation distributions (Li and Yu, 2014; Alexander et al., 2020; Contractor et al., 2021).

Contractor et al. (2021), who employ a quantile-based approach to analyze changes in precipitation distribution, suggest examining both all-day and wet-day distributions, alongside evaluating changes in the number of wet days. They note that wet-day distributions provide better insight into changes in precipitation intensity, while all-day distributions capture aggregated information on changes in both the frequency of wet days and precipitation intensity. However, caution is necessary when using wet-day distributions to analyze precipitation changes (Schär et al., 2016; Contractor et al., 2021). This is because wet-day percentiles are sensitive to changes in the number of wet days. As demonstrated by Schär et al. (2016), changes in percentile resulting from changes in the number of wet days can be misinterpreted as changes in intensity. Therefore, wet day percentile changes should not be presented in isolation from all day percentile changes, as the latter remain unaffected by variations in the number of wet days.

A gridded dataset of extreme indices with global coverage has been developed to advance research on precipitation extremes. This dataset incorporates the indices data obtained from ETCCDI's regional workshops (Dunn et al., 2020). Since its initial version, the dataset has been updated to extend the data periods and increase the number of stations. The initial version, known as the Hadley Center Global Climate Extremes Index (hereafter referred to as HadEX) (Alexander et al., 2006), was followed by GHCNDEX (Donat et al., 2013a) and HadEX2 (Donat et al., 2013b), and most recently HadEX3 (Dunn et al., 2020). One of the primary sources of daily observations used to develop these datasets of climate extremes is the daily data from GHCND (Menne et al., 2012).

HadEX3 includes 27 temperature and precipitation-based ETCCDI indices on a 1.25° × 1.875° latitude-longitude grid, covering the period from 1901 to 2018 (version 3.0.4).[1] Additionally, three more indices are included, two of which are precipitation-based and are detailed in Table 4. However, the dataset's coverage is limited across much of Africa, except for western Africa, the southernmost areas, and coastal regions near the Mediterranean. Similarly, the Arabian Peninsula, central and eastern Asia, and northern parts of South America also have sparse station representation in HadEX3.

Dunn et al. (2020) discuss discrepancies that can be observed in local extreme behaviors based on how the interpolation to the grids is made. One of two possible approaches could be used: one can either interpolate the daily precipitation data to the grids first and then compute the extreme indices, or first compute the extreme indices from the daily precipitation data and then interpolate these indices. While more research on the effects of the gridding order is necessary, Dunn et al. (2014) indicate the primary determinants of the overall analysis are the station coverage and the gridding methodology applied. In regions with adequate station coverage, there is less susceptibility to the effects of employing different gridding methodologies (Dunn et al., 2014).

Table 4
HadEX3, similar to earlier versions, includes two more precipitation-based indices: R95pTOT and R99pTOT (Dunn et al., 2020).

ID	Indicator Name	Indicator Definitions	Units
R95pTOT	Contribution from very wet days	100 * R95p / PRCPTOT	%
R99pTOT	Contribution from extremely wet days	100 * R99p / PRCPTOT	%

[1] https://catalogue.ceda.ac.uk/uuid/115d5e4ebf7148ec941423ec86fa9f26

Conversely, Herold et al. (2017) observe that the order of gridding has a significant effect on RX1day when investigating the sensitivity of extreme precipitation to different grid resolutions. Reversing the gridding order nearly eliminates the expected positive correlation between RX1day detection and grid resolution (Herold et al., 2017), while R10mm shows no sensitivity to change in gridding order (Herold et al., 2017).

4. Observed changes in extreme precipitation

The majority of existing studies on precipitation extremes have used data starting from 1950 or later, as daily precipitation data are more limited in terms of completeness, quality, and homogeneity (Alexander et al., 2019, Contractor et al., 2021). In many IPCC-linked studies, regions such as large parts of Africa, the Arabian Peninsula, and South America have poor station coverage (Benestad et al., 2019; Zhang and Zhou, 2019; Dunn et al., 2020; Sun et al., 2021; Contractor et al., 2021). A summary of the gauge-based regional studies on precipitation extreme trends is presented in Table 5 and Appendix B. Most of the studies use RClimDex (Zhang and Yang, 2004) for data quality control and calculation of the ETCCDI indices, and RHtest (WMO, 2009) for data homogenization. RHtests_dlyPrcp is specifically designed for the homogenization of daily precipitation data (Wang and Feng, 2013). Before moving on to the review of extreme-based regional studies, we briefly overview the two extreme-based global studies, Dunn et al. (2020) and Sun et al. (2021), and their findings on long-term extreme trends.

Employing the HadEX3 extreme dataset, Dunn et al. (2020) evaluate trends and changes in extreme indices on a global scale. Their findings show a significant increase in R95pTOT and RX1day trends globally over the period 1900–2018, while a non-significant increase in R10mm is also evident. However, when examining the global time series over the shorter period from 1950 to 2018, all three indices —R95pTOT, RX1day, and R10mm—show significant increasing trends (Dunn et al., 2020). Furthermore, areas illustrating significant increasing and decreasing trends show good correspondence between extremes (Dunn et al., 2020) and long-term precipitation totals (Fig. 2, section 2). This spatial correlation suggests that changes in extremes are largely responsible for observed changes in total precipitation.

Sun et al. (2021) analyze extremes (RX1day and RX5day) during 1900–2018 based on some of the datasets used to develop HadEX2 (Donat et al., 2013b), and incorporate additional stations from Argentina, China, Russia, Australia and Canada. Nonetheless, large parts of Africa, southwest Asia, South America, and central and northern Australia have poor station coverage. The coverage of the stations employed in the development of HadEX3 (Dunn et al., 2020) is greater than that used by Sun et al. (2021), particularly over South America and western and northern Africa. Sun et al. (2021) indicate a higher percentage of their stations exhibits increasing trends in RX1day and RX5day globally. Specifically, 66 % of the stations exhibit increasing trends for RX1day, compared to 34 % showing decreasing trends. Significant increasing trends in RX1day are evident at 9.1 % of the stations, while significant decreasing trends are recorded at 2.1 % of the stations (Sun et al., 2021).

4.1. Africa

Gauge-based studies focusing on observed trends in precipitation extremes across African regions are undoubtedly hindered by extensive data limitations, as is the case with studies examining precipitation totals. Most studies use a disproportionately small number of stations relative to the area under investigation, and the spatial distribution of these stations is often biased. To address gaps in daily gauge records, some extreme-based studies have relied partly or entirely on model and reanalysis data (such as Chaney et al., 2014, Teshome et al., 2022). Others have focused on evaluation of model performances and future

Table 5
Summary of gauge-based extreme studies related to African regions.

Study	Spatial coverage	Dataset	Data Period	Extreme metrics	Method	Key findings or
					Trend slope and significance	significant trends (at $P < 0.05$)
Omondi et al. (2014)	Greater Horn Africa (GHA)	station data	1971–2010	ETCCDI indices	Theil–Sen estimator (Sen, 1968)	mixed trends, mostly non-significant
Harrison et al. (2019)	"quality areas" of sub-Saharan Africa (SSA)	REGEN	1950–2013	ETCCDI indices	Theil–Sen estimator (Sen, 1968); Man-Kendal (Mann, 1945, Kendall, 1962)	significant increasing RX1day trend over wet subset; significant decreasing seasonal CDD trend over dry subsets.
McBride et al. (2022)	South Africa	station data	1921–2020	User defined thresholds based on local climate	Chi-squared (χ^2) test; Probability density function of gamma distribution.	Significant increase in probability of >50 mm, >75 mm and >115 mm precipitation, increases in frequencies of rare extremes (1-in-100 year).
Kruger and Nxumalo (2017)	South Africa	station data	1921–2015	ETCCDI indices	–	Significant increase in R95p, RX1day, particularly over southern sections of South Africa,
Donat et al. (2014)	Arab region (including parts of Africa)	station data	1960–2010	ETCCDI indices	Least squares regression.	mixed trends, mostly non-significant; significant increase (PRCPTOT and R10mm) over west African sections.

projections (such as Crétat et al., 2014, Gibba et al., 2019, Onyutha, 2020, Akinsanola et al., 2021, Ageet et al., 2022). These studies fall outside the scope of this review.

The study by Omondi et al. (2014) examines precipitation and temperature extremes across ten countries in the Greater Horn of Africa (hereafter referred to as GHA) generally over the period 1971–2010, though the data period varies among the countries based on data availability (Omondi et al., 2014). The findings by Omondi et al. (2014) show mixed trends in extreme across the GHA during the period 1971–2010, most of which are statistically non-significant. However, significant trends are found at a few stations; for instance, PRCPTOT at Asmara (1971–2010) and RX5day at Khartoum (1960–2000) both show significantly decreasing trends, while the Dodoma station (1960–2000) exhibits a significantly increasing trend in R95p. The IPCC's (IPCC, 2021) reference to Omondi et al. (2014) as evidence for increasing precipitation extremes over the GHA seems hardly fitting. It is worth noting that Omondi et al. (2014) use data from a limited number of stations (73 stations) to represent an area as vast as the GHA, with some countries, like Somalia, having no stations. Furthermore, extremes that have occurred after 2006 are not accounted for.

Gebrechorkos et al. (2018) examine temperature and precipitation extremes over three east African countries—Ethiopia, Kenya and Tanzania—over the period 1981–2016. Gebrechorkos et al. (2018) base their analysis on the CHIRPS dataset (Funk et al., 2015b), which they find to outperform three other datasets across the region in their earlier study (Gebrechorkos et al., 2017). Nonetheless, among these datasets used for the CHIRPS performance evaluation, one is a hybrid of reanalysis data and another one is entirely based on model simulation.

Numerous studies (including Dinku et al., 2018, Harrison et al., 2019, Chen et al., 2020, Cavalcante et al., 2020, Macharia et al., 2022, López-Bermeo et al., 2022, Ageet et al., 2022, Zhang et al., 2022, Han et al., 2023) document variations in the performances of the CHIRPS dataset across resolutions, regions, seasons and extreme indices. While the use of satellite rainfall products is expected in regions with scarce ground observations, it is important to emphasize that applying these datasets does not guarantee accuracy levels comparable to station data. Therefore, when discussing their advantages, it is important to exercise caution to avoid misleading policy makers or distracting initiatives aimed at increasing station coverage and access to *in situ* data. To shed more light on the uncertainty, we evaluate the performance of CHIRPS precipitation estimates using selected stations from Ethiopia in Appendix D.

According to Gebrechorkos et al. (2018), in the context of country average, the trends in annual extreme indices related to precipitation are non-significant over Tanzania during 1981–2016. CDD shows a significant decreasing trend in Ethiopia, while SDII, R95p, and R99p demonstrate significant increasing trends in Kenya. The findings for Ethiopia by Gebrechorkos et al. (2018) differ from those of Wubaye et al. (2023), who report increasing trends in most precipitation-based annual indices over Ethiopia during 1986–2020. Although Wubaye et al. (2023) use *in situ* data, their analysis is not grid-based; instead, regional averaging is conducted through direct averaging of indices at the station level. A station-based analysis may introduce biases from uneven station distributions (Zhan et al., 2018; Contractor et al., 2021; Ren et al., 2023), which is an issue in Wubaye et al. (2023). The findings of Gebrechorkos et al. (2018), showing generally non-significant trends in extreme precipitation over the three East African countries, supports the finding of Omondi et al. (2014) for GHA, despite the difference in data periods. Due to insufficient data and studies, IPCC (2021) expresses low confidence regarding changes in extreme precipitation over NEAF and SEAF regions (IPCC's reference regions corresponding to GHA, Appendix C).

In another study, Harrison et al. (2019) employ the REGEN dataset (Contractor et al., 2020) to assess changes in precipitation extremes across sub-Saharan Africa (hereafter referred to as SSA) during 1950–2013. To provide further context for their findings, Harrison et al. (2019) resolve SSA into dry, intermediate, and wet areas, with areas that have relatively good station coverage (referred to as "quality areas") receiving specific attention (Fig. 5–a) (Harrison et al., 2019). Their findings indicate a decreasing trend in PRCPTOT over both SSA and the "quality areas," with this trend being significant over the wet and intermediate subsets of the "quality areas" (Fig. 5–b). On the other hand, RX1day exhibits an increasing trend over "quality areas," with the trend being significant over the wet subsets (Harrison et al., 2019). During the season comprising the three wettest local months, R1mm (number of days with precipitation $\geq$1 mm) shows a significantly decreasing trend over the "quality areas," particularly over the intermediate subset. CDD exhibits a significantly decreasing trend over the dry subset of the "quality areas".

The "quality areas" identified by Harrison et al. (2019) include South Africa, central western Ethiopia, southern Kenya, central Zambia, Malawi, and southern West Africa. Nonetheless, with the exception of South Africa, the IPCC (2021) classifies the SSA as having inadequate data and evidence to sum up trends in precipitation extremes. Harrison et al. (2019) also point out that the "quality areas" constitute small areas that are broadly scattered across SSA and cover only about 15 % of the region. This leaves large portions of central, central-west, and northern SSA unrepresented. Put another way, analyses based on the "quality areas" are not sufficient for drawing conclusions about the entirety of SSA. Moreover, due to the sparse gauge networks, analyses considering the low-quality areas of SSA should also not be used to draw broad conclusions.

McBride et al. (2022) compare two periods, from 1921 to 1970 (period I) and from 1971 to 2020 (period II), to analyze changes in extreme precipitation occurrences over South Africa, a relatively well-gauged country in Africa. According to McBride et al. (2022), all stations have at least 90 % of the complete daily data available for the

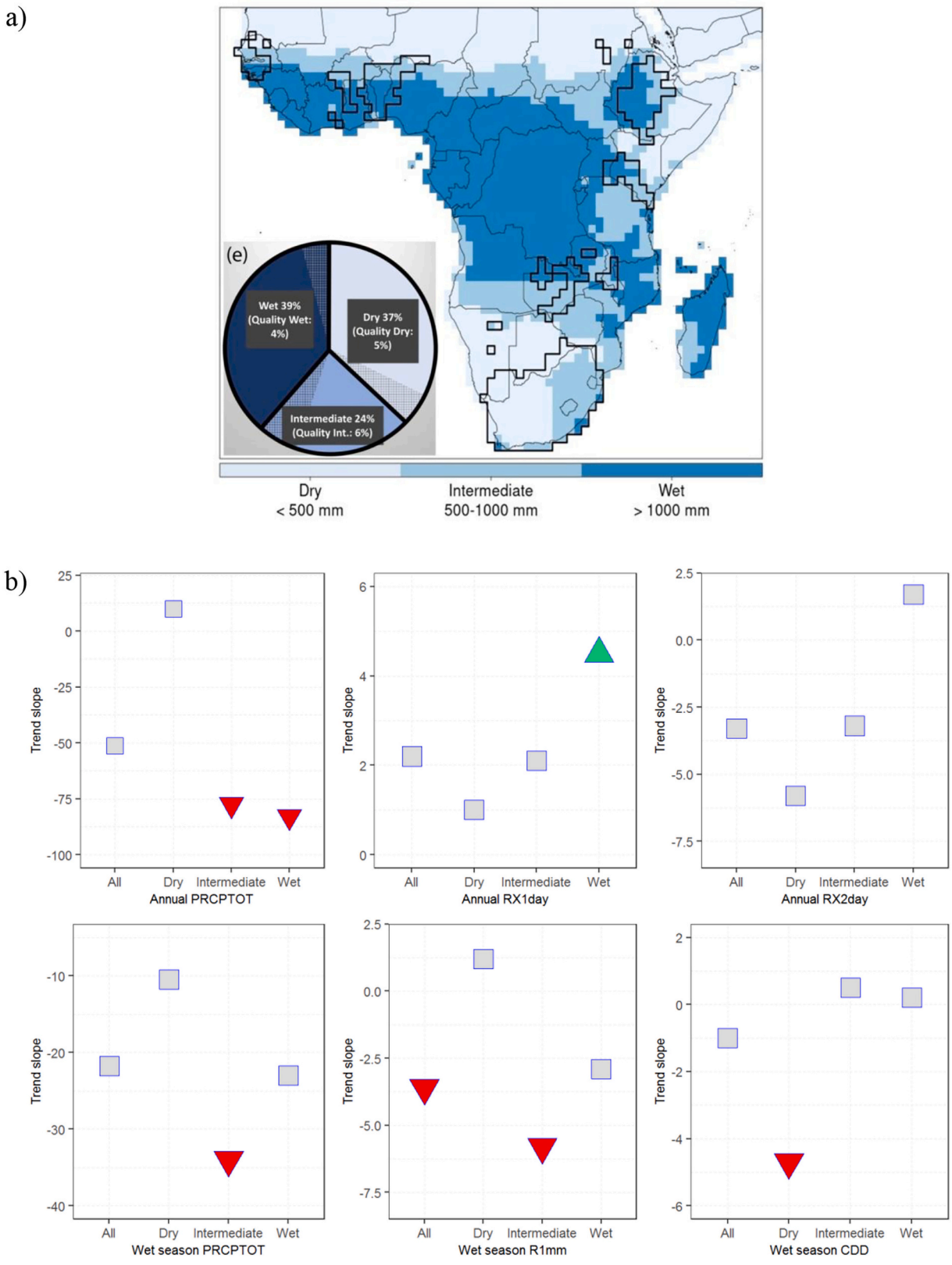

Fig. 5. (a) Dry, intermediate, and wet subsets of sub-Saharan Africa and the "quality areas" are delineated with bold black lines (from Harrison et al. (2019)); (b) computed trends and significance for the indices (1950–2013): grey squares represent non-significant trends, upward-pointing green triangles represent significantly increasing trend, and downward-pointing red triangles represent significantly decreasing trends (based on findings by Harrison et al. (2019)). (For interpretation of the references to colour in this figure legend, the reader is referred to the web version of this article.)

period. Their results indicate a 4 % increase in "heavy or extreme" (≥50 mm) precipitation between the two periods (McBride et al., 2022). For majority of the stations in the country, higher probabilities of experiencing precipitation exceeding 50 mm, 75 mm, and 115 mm on wet days are found during period II compared to period I (McBride et al., 2022). While South Africa has seen significant increases in precipitation extremes, including an increase in frequency of rare extremes, trends can exhibit spatial variability (Kruger and Nxumalo, 2017, McBride et al., 2022).

The findings of McBride et al. (2022) align with the IPCC (2021) assessment over southern Africa, which indicates increasing trend in precipitation extreme events since 1950. South Africa is located in the southern sections of the WSAF and ESAF reference regions (as defined by the IPCC, Appendix C). For both reference regions, Sun et al. (2021) report increases in both RX1day and RX5day during 1950–2018. Based on HadEX3, Dunn et al. (2020) identify a significantly increasing trend in RX1day in certain areas of ESAF, while trends are non-significant over the WSAF region.

For northern Africa, Donat et al. (2014) demonstrate that trends in extremes during 1960–2010 are mixed and lack spatial coherence, with most being statistically non-significant. Exceptions to this are stations in the west African sections of the study area (near 20°N) for the period 1981 onwards, where significant positive trends in PRCPTOT and R10mm are evident (Donat et al., 2014). Notably, Dunn et al. (2020) show a significant decreasing trend in R10mm over west Africa, in contrast to Donat et al. (2014), but using a longer data period (1950–2018).

4.2. Other regions

Asia. Choi et al. (2009) observe that trends in extremes are generally non-significant and spatially incoherent across the Asia-Pacific Network Region (APN), which includes China and Australia, during 1955–2007. Similarly, Dunn et al. (2020) find a generally non-significant trend in RX1day across much of Asia during 1950–2018, with the exception of eastern Asia and southern India, where significant increases are evident. Sun et al. (2021) have also identified a comparable regional pattern in RX1day across Asia, excluding southern Asia and the Arabian Peninsula. The R95PTOT exhibits a largely non-significant trend over a substantial portion of the continent, with significant increases observed only in eastern Asia (Dunn et al., 2020). Moreover, there is a notable increasing trend in R10mm over Northeast Asia and some parts of western Asia (Dunn et al., 2020). Previous studies, such as Zhou et al. (2016), report a modest increase in some extreme indices over China, while the IPCC (2021) indicates that extreme trends are non-significant. Nonetheless, Zhang et al. (2020) highlight that biases lead to underestimation and reveal considerable increases in annual rainstorm during 1961–2010 after adjustments are made.

Europe. Comparing two periods, 1951–1980 and 1984–2013, Myhre et al. (2019) illustrate positive changes in extreme precipitation over Europe using percentile-based extreme indices from R95p to R99.99p. They find that the magnitude of change increases with higher percentiles. According to Myhre et al. (2019), the contribution from changes in frequency is significant compared to changes in intensity. Similar to the findings by Myhre et al. (2019) regarding rare extremes, Van Den Besselaar et al. (2013) report significant changes in extreme events occurring once every 10 and 20 years during 1951–2010. Dunn et al. (2020) and Sun et al. (2021) find significant increasing annual trends in RX1day and RX5day over northern Europe during 1950–2018. Similarly, Myhre et al. (2019) demonstrate predominantly positive changes in R99p across northern Europe for the period 1951–2013, while Zeder and Fischer (2020) indicate an increasing trend in RX1day over central Europe over the long-term (1901–2013).

North America. Since 1980, single–day precipitation extremes show a significant increasing trend averaged over the United States (EPA, 2022). Hoerling et al. (2016) illustrate a significant increasing trend in R95p over the Northeast climatic region during 1979–2013, while observing a significant decreasing trend over the West climatic region. A comparable spatial pattern is reported in the long-term R95p trend (1901–2013), with an increase in the northeastern United States and a decrease in the southwestern United States (Hoerling et al., 2016). Powell and Keim (2015) find increasing trend in R95p at most stations across the southeastern United States over the period 1948–2012. Conversely, Hoerling et al. (2016) report a non-significant decreasing trend in R95p over the southern and southeastern regions of the United States, including the region analyzed by Powell and Keim (2015). The discrepancy in the results may be due to the differing data periods: about 65 years for the analysis by Powell and Keim (2015) and 35 years for Hoerling et al. (2016). Supporting the findings of Powell and Keim (2015), Dunn et al. (2020) illustrate significant increasing trend in R95pTOT across the southeastern United States over the period 1950–2018.

Yang et al. (2019) report significant increasing trends in extreme indices, including RX1day, RX5day, and R95p, over Canada during 1950–2012. Vincent et al. (2018) find that the number of days with rainfall greater than the 90th percentile increases by an average of 1.3 days nationwide. They also show a significant increasing trend in heavy rainfall over the eastern areas of southern Canada, southern Quebec, and many places in British Columbia during 1948–2012. Despite these findings, Vincent et al. (2018) note that most of southern Canada experiences decreasing heavy snowfall trends during the same period, although these trends are not as pronounced as those for heavy rainfall. However, the country's central and northern regions exhibit increasing trends in days with heavy snowfall (Vincent et al., 2018).

South America. According to de los Milagros Skansi et al. (2013), increasing trends in RX1day, RX5day and R99p are evident over South America during 1950–2010, though these trends are largely non-significant. Although the station coverage by de los Milagros Skansi et al. (2013) is an improvement over the earlier work by Haylock et al. (2006), large areas of Brazil, southern Argentina, and Uruguay have inadequate station coverage. Da Silva et al. (2019) find mostly non-significant trends for extreme indices over the Amazon Basin and northeast Brazil during 1980–2013. Similarly, a largely non-significant trend in RX1day is depicted by Dunn et al. (2020) over the Amazon Basin. However, they identify a significant increasing trend over southern Brazil, Uruguay, and northern Argentina, contrasted by a significant decreasing trend in Chile and northeastern Brazil (Dunn et al., 2020).

Australia. Choi et al. (2009) and Alexander and Arblaster (2017) observe that trends in extremes over Australia are generally non-significant over different periods, 1911–2010 and 1955–2007, respectively. Alexander and Arblaster (2017) find significant decreasing trends in SDII and CDD on average over Australia. Choi et al. (2009) report that a larger proportion of stations exhibit increasing trend in R95p over western Australia, while eastern Australia experiences decreasing trend in R95p. Dunn et al. (2020) depict a similar spatial pattern for trend in R95pTOT during 1950–2018, along with a significant increasing trend in R1xday over western Australia. Contractor et al. (2018) report negative changes in the number of wet days over eastern and southern Australia comparing two periods, 1958–1985 and 1986–2013, especially during March–May and September–November seasons. A high spatial correlation between precipitation totals and extremes across Australia is previously reported by Alexander et al. (2007).

5. Status quo of station coverage and precipitation data over Africa

Africa, a continent of immense size and diversity, hosts a variety of intricate landscapes and rich ecosystems (Monadjem, 2023), showcasing a broad spectrum of weather and climate patterns (Hulme et al., 2001; Giannini et al., 2008; Bekele-Biratu et al., 2018; Nicholson, 2019; Le Coz and Van De Giesen, 2020; Palmer et al., 2023). Despite its significance as

a global weather and climate driver and its vulnerability to climate variability and change, Africa faces challenges in providing sufficient precipitation data necessary for understanding long-term climate trends and variability (Dinku, 2019; IPCC, 2022). It remains one of the least covered regions (Dezfuli et al., 2017; Le Coz and Van De Giesen, 2020; Kaspar et al., 2022), accounting for an estimated 10 % of the global climate station coverage (IPCC, 2022). The station coverage is particularly sparse in rural and remote areas, leading to an uneven distribution of stations across the continent (Dinku, 2019; Muthoni et al., 2019). Compounding the issue of an already limited station network, the number of operational stations in Africa has steadily declined over the past few decades (Nicholson et al., 2018; Dinku, 2019; Bliefernicht et al., 2021; IPCC, 2022).

Notably, areas like southern Africa exhibit better spatial and temporal coverage (Kidd et al., 2017, Kruger and Nxumalo, 2017, Harrison et al., 2019, Contractor et al., 2020, McBride et al., 2022). Examining the spatial coverage of climate stations along with their operational duration and consistency is also necessary, as this provides deeper insight into the data challenges. In this regard, the spatial coverage of the stations over Africa in the REGEN dataset illustrated by IPCC (2022) is an aggregate, and could exhibit significant thinning when analyzed over distinct time periods, as shown by Contractor et al. (2020). Despite efforts at regional and international levels to improve the coverage of observational stations in Africa, progress remains limited, hindered by additional factors such as conflicts and inadequate funding (Dezfuli et al., 2017, Dinku, 2019, Al-Zu'bi et al., 2022, IPCC, 2022). As a result, many areas of the continent continue to lack adequate meteorological station coverage.

African stations that supply daily precipitation data to the GHCND dataset (Table 1) are shown in Fig. 6. While the actual station coverage may be different from this, as demonstrated by Ethiopia's situation in Fig. 7, the distribution of GHCND stations illustrates the sparse coverage over the continent, particularly before1950. A similar illustration of the spatiotemporal coverage of GPCC stations across Africa is not produced as the GPCC data (Table 1) is provided in grid fields, and the latitude-longitude details of the stations and the duration of their data are not available. However, examining the spatial coverage of stations supplying data for a certain month or day can give a glimpse of the coverage of GPCC stations over Africa, as shown by Sun et al. (2017) for July 2005 and Dinku (2019) for July 2013. As GPCC gathers more stations than GHCND, improvement in coverage is noted, however considerable areas remain sparse, particularly across the northern and central remote areas of the continent. Besides, Africa lacks precipitation data for the most recent years in the GPCC (Dinku, 2019; Schneider et al., 2022a).

Similarly, Africa has poor station coverage in other available gridded gauge-based climate datasets (Alexander et al., 2019; Dunn et al., 2020; Contractor et al., 2020; Ziese et al., 2020; Harris et al., 2020). For instance, REGEN, a global daily dataset identified by Contractor et al. (2021) as having the highest density of stations, has meaningful station coverage over southernmost areas of Africa and is mostly limited to the years 1950–1999 (Contractor et al., 2020). In addition to the insufficient gauge networks on the ground, the limited representation of Africa in the REGEN dataset is linked to countries' willingness to share observations (Contractor et al., 2020). Moreover, the number of stations has varied over time or declined recently in several global datasets, which presents an additional challenge to the long-term precipitation assessments (Funk et al., 2015a; Sun et al., 2017; Dinku, 2019; Alexander et al., 2019; Contractor et al., 2020; Schneider et al., 2022a). In addition to direct precipitation data from the station-based and grid-based datasets, computed indices are also available on grid fields. As discussed in section 3, one such product with global coverage is HadEX3, the recent version of HadEX. However, the stations used to develop HadEX3 have limited spatial coverage over Africa.

To further demonstrate the challenge, the case of Ethiopia is presented based on the metadata of all the national meteorological stations acquired from the Ethiopian Meteorological Institute (EMI). There are

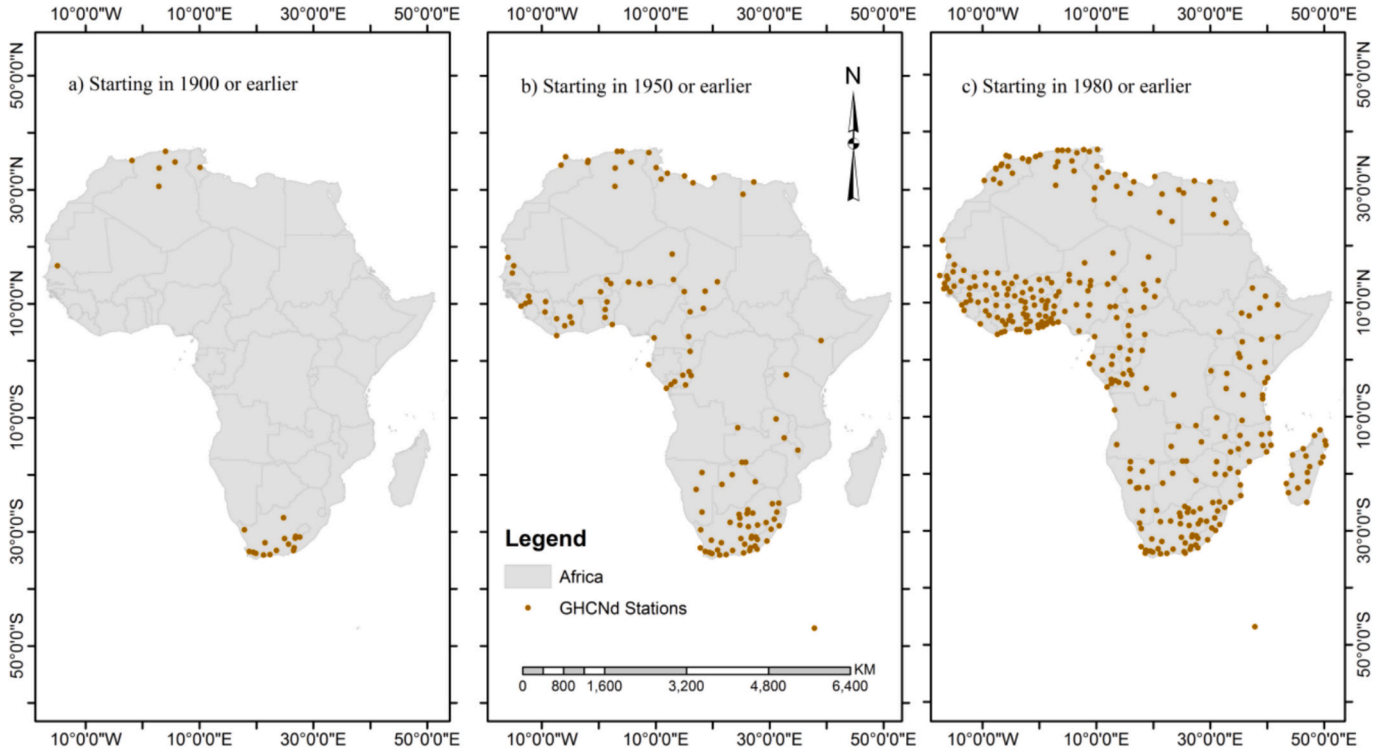

Fig. 6. African stations that are part of GHCND and have a data period a) starting in 1900 or earlier b) starting 1950 or earlier and c) starting in 1980 or earlier. All the stations shown here have data ending in 2020 or later, while information on missing records is not indicated. Information about the stations is available at NOAA's National Center for Environmental Information.
https://www.ncei.noaa.gov/products/land-based-station/global-historical-climatology-network-daily

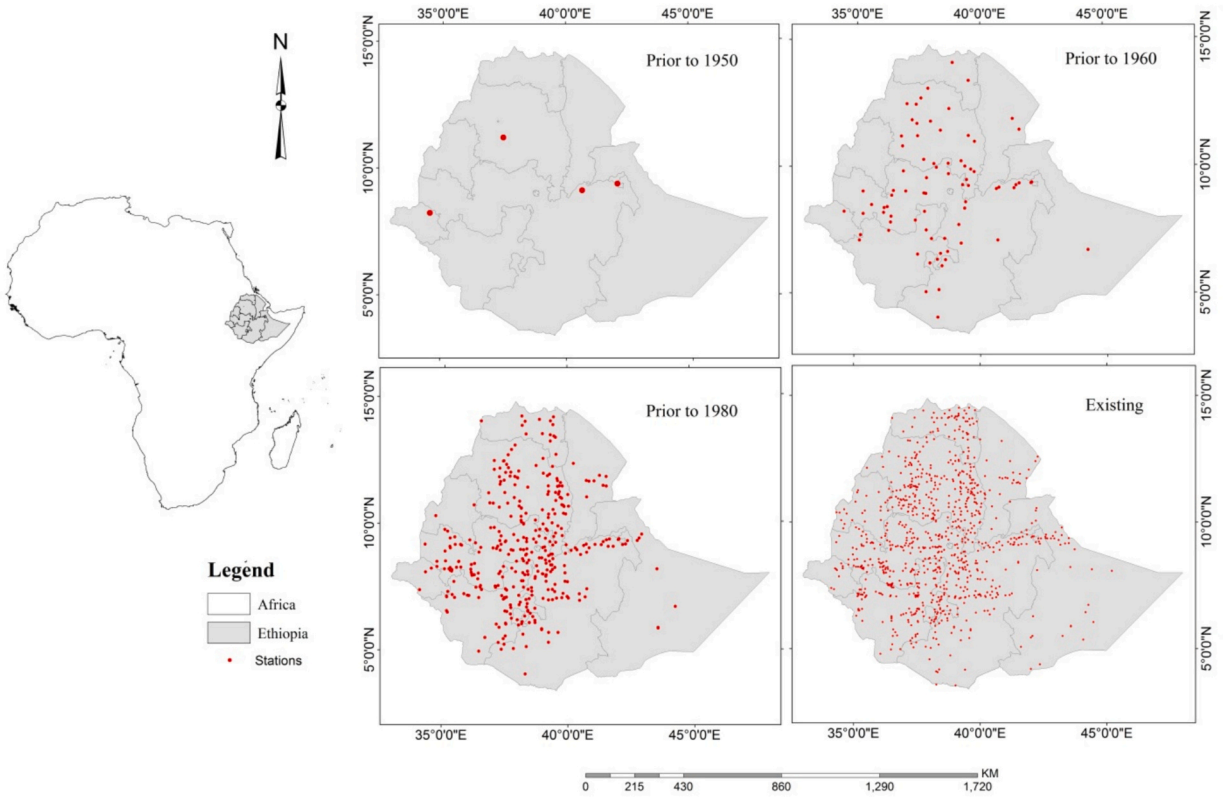

Fig. 7. The spatial coverage of meteorological stations in Ethiopia (East African country) in the periods prior to 1950 (top-left), prior to 1960 (top-right), prior to 1980 (bottom-left) and present (bottom-right).

just four stations that have been operational prior to 1950, as seen in Fig. 7. The number of stations increases between 1950 and 1960, particularly across the central regions of the country. While little progress is noted in the following decade, 1960–1970, a significant increase in the number of stations in Ethiopia occurs before 1980, with most new additions again concentrated in the central regions. The bottom right panel of Fig. 7 shows the spatial coverage of existing stations across Ethiopia, including a few stations that have ceased observation. Large areas of eastern and southeastern Ethiopia are sparsely covered, and border regions, which are typically rural, remain to have inadequate coverage. In addition to the sparse spatial distribution of stations, as is common in most African nations, issues related to data completeness are typical (Dinku, 2019; Dufera et al., 2023; Mena et al., 2023).

Sparse station coverage has caused disparities across different datasets in the representation of precipitation in African regions, while values are generally consistent in other global regions with better station coverage (Sun et al., 2017; Zittis, 2018; Dosio et al., 2021). Using merged gauge-satellite datasets is suggested to reduce the disparities in precipitation values arising from the limited station coverage (Parker et al., 2011; Novella and Thiaw, 2013; Dinku et al., 2018; Kaspar et al., 2022). Nonetheless, the blending of observations with satellite products or reanalysis data to bridge this gap poses further limitations stemming from estimation algorithms and model uncertainties (Zhang et al., 2011, Sun et al., 2017, Harrison et al., 2019, Alexander et al., 2019, Le Coz and Van De Giesen, 2020, Alexander et al., 2020, Dosio et al., 2021, Al-Zu'bi et al., 2022). Daily or sub-daily precipitation, in particular, is the most difficult to replicate (Ombadi et al., 2021; Kagone et al., 2023; Mekonnen et al., 2023). The limitation is compounded by the need for *in situ* data in the development of these products (Kagone et al., 2023, Mekonnen et al., 2023). Besides, satellite precipitation datasets often cover short periods that mostly begin in 1980 or later (Sun et al., 2017; Contractor et al., 2021). Because of this, their availability for long-term precipitation assessment—like centennial trend analysis—is limited. Similarly, with considerable disparities among them, reanalysis products lack the precision needed to reliably fill long-term data gaps and remain a work in progress (Alexander et al., 2020; Dosio et al., 2021).

In addition to sparse station coverage, it is important to underline the issues related to data quality, homogeneity, and the frequency of missing records, which present significant challenges. Encountering quality issues, stemming from observing and archiving practices that do not conform to the WMO standard (WMO, 2008), is not rare in Africa (Dinku, 2019, Al-Zu'bi et al., 2022, Bliefernicht et al., 2021). It is also common to find data having short periods or several missing records, particularly in daily precipitation series (Omondi et al., 2014; Kruger and Nxumalo, 2017; Dezfuli et al., 2017; Dinku, 2019; Dufera et al., 2023). Data inhomogeneity frequently arises from changes in station locations caused by instabilities, construction, and urbanization. By demonstrating the disparity between historical trends calculated using homogenized data and raw data, Wang et al. (2023) provide strong evidence for the need to ensure homogeneity in observations before their use.

The lack of data over Africa is also a result of further issues related to restrictive data policy, inadequate maintenance and calibration, and the inaccessibility of non-digitized data archives (Dezfuli et al., 2017; Dinku, 2019; Bliefernicht et al., 2021; Kaspar et al., 2022; IPCC, 2022). Since countries enforce stern data policies that restrict access, the actual precipitation data that is available in Africa is thought to differ from the data shared with the WMO and used in global datasets (Donat et al., 2013b; Dezfuli et al., 2017; Nicholson et al., 2018; Dinku, 2019; Dunn et al., 2020; Contractor et al., 2021). For instance, according to Deutscher Wetterdienst (producer of GPCC[2]), no African nation is seen in the country list that contributed precipitation data to GPCC between

[2] https://www.dwd.de/EN/ourservices/gpcc/editorial/latest_datadeliveries.html?nn=495490

2019 and 2023, nor are there any African stations with data extending beyond 2016. The same can also be observed in the cases of Uganda, Mali, Madagascar and Rwanda, as illustrated by Dinku (2019). Due to poor maintenance and funding limitations, some observational stations in Africa operate with outdated equipment or encounter technical issues that produce incomplete or unreliable data. Another factor in certain countries has been the lack of established mechanisms for exchanging data with regional or global organizations (Dinku, 2019).

Some national meteorological services have non-digitized data, which is therefore not readily available to be shared (Dinku, 2019). In some circumstances, data archives can be located in different places or even not known (Brönnimann et al., 2018; Kaspar et al., 2022). The International Data Rescue (I-DARE)[3] portal served as a centralized platform that provides information and metadata on projects working on data rescue, the progress of climate data digitization, and data that still requires digitization. The WMO's Commission for Climate Expert Team on Data Rescue, which falls under Global Framework for Climate Services (GFCS), oversaw I-DARE, while the Royal Netherlands Meteorological Institute (KNMI) operated the portal. The I-DARE portal highlighted projects worldwide aligned with these objectives. Notably, Africa ranked second after Europe in the number of Data Rescue (DARE) projects (Brunet et al., 2020). Nonetheless, many of these projects concentrated on specific regions, primarily coastal areas in western, equatorial eastern, and southwestern Africa (Brunet et al., 2020). This suggests that other regions on the continent may still have archives requiring digitization. Although detailed documentation on the current status of these projects is lacking, some have been completed. Following the integration of efforts between the World Meteorological Organization (WMO) and the Copernicus Climate Change Service (C3S), the International Data Rescue (I-DARE) initiative has transitioned to a new platform hosted at dataresCue.climate.copernicus.eu.[4]

6. Conclusions, suggestions and prospects

This review evaluates the extent of existing studies on precipitation changes that use *in situ* data or gauge-based datasets, how comparable they are, and how well their findings align to determine regional trends. The various causes of discrepancies in results are highlighted, along with limitations and uncertainties related to station coverage, precipitation representations, gridding order, and the applications of satellite and reanalysis products. The review also demonstrates the ongoing challenges related to the availability and accessibility of precipitation data both spatially and temporally, with particular emphasis given to Africa.

Generally, the existing gauge-based regional studies are limited and diverse. There are limited recent studies assessing long-term precipitation trends that account for continental territories, even for continents with good station coverage. The regional studies exhibit complex differences in data period, analysis region, methods, precipitation metrics, and the type of datasets used. As a result, comparing findings to generalize regional precipitation trends is very difficult. The application of ETCCDI indices has played a significant role in harmonizing extreme-based studies and reducing differences arising from extreme representations. Nonetheless, differences persist as some studies selectively use certain indices to focus on specific aspects of extremes or employ alternative metrics to track significant extremes, as ETCCDI indices reflect moderate extremes. In this regard, developing indices for analyzing precipitation extremes with long return periods, as well as establishing standardized methods to examine changes across the entire precipitation distribution, could be a step forward.

This review notes that there is uneven station distribution in each continent, and that this is also mirrored in the existing global datasets. Africa stands as the most deprived continent regarding long-term precipitation records and spatial coverage. The station coverage over South America is also poor. Asia has good station coverage, especially in eastern and southern regions, but the Arabian Peninsula in western Asia lacks observations. The station coverage over the eastern half of the European continent is not adequate. Northern Canada and central Australia are also regions with sparse station coverage. Furthermore, data quality and inhomogeneity issues are shown to be the case for most continents.

Conclusions are drawn based on findings that show a reasonable agreement among regional studies with comparable analysis region and data periods. Despite studies examined in this review revealing heterogeneous and mostly non-significant local trends, due to insufficient data and lack of robust evidence, the long-term precipitation trend remains largely undetermined across most of Africa, with slight exceptions in the northern, southern and western areas of the continent. There is a clear implication that a precipitation trend depiction for Africa based on continental average is likely to be inappropriate. There are relatively more references on northern Africa available as it has added coverage from studies focusing on Mediterranean regions, and the findings of these studies are generally consistent. South Africa has preserved long-term instrumental data, and has thus been the subject of thorough analysis, though studies on centennial precipitation total trends are inadequate. A generally non-significant decreasing trend in precipitation total is evident over northern Africa over the past century, while a few studies agree that there is a significant decreasing trend recorded in sections of western Africa. Significant increasing trend in precipitation extreme, and frequencies of rare extremes, is evident over South Africa.

Over the past 120 years, Asia's average annual precipitation total has increased significantly, and since 1950, the continent has consistently seen positive average precipitation anomalies. From a sub-region perspective, the increases in long-term precipitation totals dominate over northern Asia and the western parts of central Asia, while the increases are most evident for the winter, autumn, and spring seasons. Trends in precipitation extreme, like RX1day, over Asia have primarily been non-significant since 1950. However, significant increasing trends in RX1day and R95PTOT are evident over eastern Asia. The majority of northern and western Europe has experienced considerable increases in annual precipitation total over the past century, while it has generally decreased over southern Europe. Reflecting the spatial patterns of long-term total trends, significant increases in extreme trends like RX1day, RX5day, and R99p are observed in northern and central Europe since 1950, with rare precipitation extremes becoming more frequent.

Since there is insufficient data in northern Canada, particularly before 1950, studies focus on southern Canada to analyze centennial precipitation trends. During the 20th century and into the 21st century, annual precipitation has demonstrated increases over southern Canada, with significant increases in the eastern and western regions. Many extreme indices demonstrate significant increasing trends across Canada since 1950. Conversely, heavy snowfall exhibits a downward trend across southern Canada. The long-term precipitation total has also generally increased in the United States, with significant increasing trends prevailing in the eastern regions. Increasing trends in precipitation extremes, such as RX1day, R95pTOT and R10mm, are evident over northeastern United States since 1950. The long-term precipitation total has significantly increased in the southeastern region of South America. Since 1950, trends in precipitation extremes over the Amazon basin have been non-significant. Across most of Australia, long-term annual precipitation generally shows a slight upward trend, with increases being more pronounced over central-northern Australia. Trends in precipitation extreme are predominantly non-significant across Australia, while a significant increasing trend in R1xday is observed in western Australia.

It is very crucial that African countries ease restrictions to allow abundant access to precipitation data. As the existing stations used in global datasets do not fully represent the actual number of stations in

[3] https://www.knmi.nl/research/observations-data-technology/projects/the-international-data-rescue-i-dare-portal

[4] https://datarescue.climate.copernicus.eu/

Africa, it is necessary to work toward increasing the number of stations through collaborative initiatives with these nations. The three initiatives launched by the World Meteorological Organization (WMO)[5]—Unified Data Policy, the Global Basic Observing Network (GBON), and the Systematic Observations Financing Facility (SOFF)—hold a prospective promise to serve as a foundation for improving climate data accessibility in Africa. With the aim of ensuring free and unrestricted access to data, the new Unified Data Policy is believed to strengthen and promote the commitment of member states to the exchange of data.

Under its aspiration of increasing the availability of surface-based observations for global numerical weather prediction (NWP), GBON aims to address the insufficient collection of observations and the inadequate data sharing. As a continent where these issues are prevalent, Africa is expected to be among the particular focus of GBON's implementation. This is evidenced by the recent increase in African stations designated to GBON, from 589 to 1045, overseen by the WMO Regional Office for the continent,[6] and this needs to be sustained. The financial and technical assistantship promised by SOFF is vital for the African nations to uphold these commitments. The hope is that the data from these stations, monitored globally by GBON, will also be accessible to a wider user base.

To comprehend the actual spatial and temporal coverage of meteorological stations across Africa, it is essential that the stations' metadata be accessible on the websites of national meteorological service agencies, and that this information is regularly updated. Efforts should also focus on installing new stations to remarkably increase coverage across Africa. Initiatives to establish and monitor climate stations across Africa, like the Trans-African Hydro-Meteorological Observatory (TAHMO)[7] and SARCIS-DR,[8] must be supported and strengthened. In this context, national universities and research institutes can play a crucial role by installing and operating automated weather stations within their research areas, or watersheds as is the case in Ethiopia, and by maintaining their own data archives for research purposes. Initiatives aimed at enhancing precipitation prediction, such as the Global Precipitation Experiment (GPEX),[9] can play pivotal roles in supporting the establishment and monitoring of observation stations, which provide invaluable data necessary for improving prediction skills and supporting future research on regional climate change and variability.

Furthermore, there should be an increase in regional studies on precipitation changes and variability using *in situ* or gauge-based datasets, and comparable analyses regions and data periods should be taken into account. One way to achieve this could be taking the IPCC reference regions into consideration.

Declaration of competing interest

The authors declare no conflict of interest.

Acknowledgments

The authors acknowledge the support from the China University of Geosciences, Wuhan, and the Chinese Scholarship Council (2020GXZ017074). The authors also acknowledge the Editor and anonymous reviewers for their valuable comments and suggestions, which have improved this article. This study is supported by the National Key Research and Development Program of China (No.2018YFA0605603).

Appendix A. Summary of gauge-based studies on long-term precipitation total trends over various global regions other than Africa

Study	Spatial coverage	Dataset	Data Period	Precipitation metrics	Method	Areas showing significant trend (at $P < 0.05$)	
					Trend slope and significance	Significantly increasing	Significantly decreasing
Ren et al. (2017)	Hindu Kush Himalayan region	CGP1.0, assigned to 5° × 5° grids	1901–2014	precipitation standardized anomaly (PSA)	Least squares method; Man-Kendal (Mann, 1945, Kendall, 1962).	–	–
Zhan et al. (2018)	Asia	CGP1.0; RBMP; national datasets, assigned to 5° × 5° grids	1901–2016	normalized precipitation anomaly (NPA)	Linear list square method; Student's *t*-test.	north Asia (north of 50° N); north Asia and central Asia (for winter, spring and Autumn seasons)	south Asia (for winter season)
Ren et al. (2023)	Asia	CGP1.0; RBMP; national datasets, assigned to 5° × 5°	1901–2019	precipitation anomaly percentage	Theil–Sen estimator (Sen, 1968); Man-Kendal (Mann, 1945, Kendall, 1962)	high latitude regions; mid-latitude regions between 60° E and 80° E. (western section of Central Asia)	southwest India, pockets of southern southeast Asia
	China	CGP1.0; assigned to 2.5° × 2.5° grids				–	–

Study	Spatial coverage	Dataset	Data Period	Precipitation metrics	Method	Areas showing significant trend (at P < 0.05)	
					Trend slope and significance	Significantly increasing	Significantly decreasing

(*continued on next page*)

[5] https://wmo.int/news/media-centre/wmo-overhauls-data-exchange-policy

[6] https://wmo.int/media/magazine-article/africa-increases-designation-of-gbon-stations#:~:text=As%20a%20result%2C%20GBON%20stations,January%202,023 %20and%20June%202,023.

[7] https://www.metergroup.com/en/meter-environment/case-studies/tahmo-weather-stations-africa

[8] http://csc.sadc.int/en/home-side/projects/sawidra-sarcis-dr

[9] https://www.wcrp-climate.org/gpex-overview

(*continued*)

Study	Spatial coverage	Dataset	Data Period	Precipitation metrics	Method	Areas showing significant trend (at P < 0.05)	
					Trend slope and significance	Significantly increasing	Significantly decreasing
Hu et al. (2017)	northern parts of central Asia (region divided to highland and plain sub-regions)	GPCC v. 7	1901–2013	annual precipitation (mm/decade)	Linear list square method; Student's t-test.	increasing trend at both sub-regions, with the increasing trend being higher over the plain sub-regions.	–
Peña-Angulo et al. (2020)	southwestern Europe (including Spain, Portugal and Italy)	dataset developed by Vicente-Serrano et al. (2020)	1870–2018	annual total precipitation (mm/year)	Linear regression model, non-parametric Mann-Kendall test (Hamed and Rao, 1998)	–	–
Caloiero et al. (2018)	Europe and Mediterranean	GPCC v.6.0	1901–2009	annual precipitation (mm/decade)	Theil–Sen estimator (Sen, 1968); Man-Kendal (Mann, 1945, Kendall, 1962)	central and central-north Europe: Norway, Sweden, Germany, France, north-western Russia, northern United Kingdom, Netherlands and Estonia	southern European region—Italy, southern Austria, southern Spain, Albania and Greece, northern Ireland and northern outskirts of Norway.
Philandras et al. (2011)	Mediterranean	CRU version TS 3.1	1901–2009	annual total precipitation (mm/year)	Man-Kendal (Mann, 1945, Kendall, 1962)	northwestern Spain, southwestern France and southwest coastal areas of the Black Sea.	coastal areas of southern Europe, including central and northern Italy, Croatia and southern Spain

Study	Spatial coverage	Dataset	Data Period	Precipitation metrics	Method	Areas showing significant trend (at P < 0.05)	
					Trend slope and significance	Significantly increasing	Significantly decreasing
Zhang et al. (2000)	southern Canada (below 60° N)	station data, assigned to 0.45° × 0.45° grids	1900–1998	annual precipitation	Linear regression model, Zhang et al. (2000).	over southern Canada; eastern and western areas of southern Canada (for all the four seasons).	–
				annual ratio of snowfall to precipitation		over southern Canada (with an increase in precipitation during winter being the cause).	–
Vincent et al. (2018)	Canada	station data	1948–2012	number of "wet days"	methodology developed by Zhang et al. (2000), Kendall's τ-test (Kendall, 1955)	averaged over Canada; southwestern and southeastern Canada	–
				number of days with snowfall		pocket areas of northwestern and northern Canada	southwestern and southeastern Canada
Wang et al. (2023)	Canada	station data; quality controlled and homogenized datasets	1948–2012	annual total precipitation (mm/decade)	Man-Kendal (Mann, 1945, Kendall, 1962)	57 % of the grids; east and west coasts of southern Canada, northern Canada.	–
	southern Canada		1900–2019			78 % of the grids; eastern and western outskirts of southern Canada.	–
Haylock et al. (2006)	South America	station data	1960–2000	PRCPTOT	Kendall's Tau method (Kendall, 1938)	southern Brazil, Paraguay, Uruguay and northeastern Argentina, southeastern regions of South America.	southern Peru and southern Chile
de los Milagros	South America	station data	1950–2010	PRCPTOT	Kendall, 1955	southeastern regions of South America,	–

(*continued on next page*)

(*continued*)

Study	Spatial coverage	Dataset	Data Period	Precipitation metrics	Method	Areas showing significant trend (at P < 0.05)	
					Trend slope and significance	Significantly increasing	Significantly decreasing
Skansi et al. (2013)							northern South America (at $P < 0.01$)

Study	Spatial coverage	Dataset	Data Period	Precipitation metrics	Method	Areas showing significant trend (at P < 0.05)	
					Trend slope and significance	Significantly increasing	Significantly decreasing
Varuolo-Clarke et al. (2021)	Southeastern South America	CRU v. 4.04, (GPCC v2018)	1901–2019 (2016)	standardized precipitation (% / decade)	Man-Kendal (Mann, 1945, Kendall, 1962)	entirety of southeastern South America	–
Dey et al. (2019)	Australia (This is a review)		1910–2015			northern Australia	southwest and southeast Australia

Study	Spatial coverage	Dataset	Data Period	Extreme metrics	Method	Key findings or significant trends (at P < 0.05)
					Trend slope and significance	
Choi et al. (2009)	Asia-Pacific Network Region (APN)	station data	1955–2007	ETCCDI indices	Least squares method and Kendall's τ–test	non-significant and spatially incoherent, stations showing increasing and decreasing trends are proportional,
Zhou et al. (2016)	China	gridded climate dataset (Wu and Gao, 2013)	1961–2010	ETCCDI indices	Least squares method and t-test	slight increase in PRCPTOT, SDII and R95p, significantly decreasing CDD averaged over China; increasing PRCPTOT, SDII and R95p trends across western half of the country and eastern China.
Chang et al. (2020)	China	station data (hourly data)	1980–2015	precipitation accumulation cutoff scale	changes in the cutoff scale (comparing two periods)	increases in cutoff scale over 58.5 % of the stations,
Van den Besselaar et al. (2013)	Europe	ECA&D	1951–2010	Return periods	generalized extreme value (GEV) distribution is fitted	a general decrease in return periods over Europe for the extremes occurring once every 5, 10, and 20 years; significant decrease is found for the winter and spring seasons across northern Europe.

Appendix B. Summary of gauge-based studies on precipitation extreme trends over various global regions other than Africa

Study	Spatial coverage	Dataset	Data Period	Extreme metrics	Method	Key findings or significant trends (at P < 0.05)
					Trend slope and significance	
Myhre et al. (2019)	Europe	E–OBS	1951–2013	R95p, R99p, R99.7p, R99.9p, R99.95p, R99.99p,	computing changes between 1951–1980 and 1984–2013	positive changes, with the magnitudes being large for higher percentiles; significantly positive change in R99p over northern Europe; greater increase in frequency of rare extreme events than increase in intensity.
Zeder and Fischer (2020)	central Europe, comprising Germany, Netherlands, Austria and Switzerland.	station data	1901–2013	RX1day, RX3day, RX5day, RX7day	Theil–Sen estimator (Sen, 1968); Man-Kendal (Mann, 1945, Kendall, 1962)	increasing RX1day trend in more proportion of stations; significant increasing RX1day trend across western and south western sections;
Hoerling et al. (2016)	United States	GHCND, gridded to 0.94° × 1.25° fields	1979–2013	R95p	linear method,	increasing R95p trend dominate northern and northeastern, while decreasing trend dominate southern and western regions;
Powell and Keim (2015)	Southeastern United States	USHCN (Menne et al., 2015)	1948–2012	ETCCDI indices	Least squares method, *t* test, Principal component analysis (PCA)	increasing trend in more proportion of stations; significant increasing R95p and R20 trends at 10 % and 9 % of the stations, respectively; significant decreasing CWD trend at 72 % and 17 % of the stations; spatially non-coherent trends over the region.

Study	Spatial coverage	Dataset	Data Period	Extreme metrics	Method	Key findings or significant trends (at P < 0.05)
					Trend slope and significance	
Vincent et al. (2018)	Canada	station data	1948–2012	number of days with rainfall >90th percentile	methodology developed by Zhang et al. (2000), Kendall's τ-test (Kendall, 1955)	increase by 1.3 days nationwide on average; with significant trends across the eastern outskirts, southern Quebec, and many places in British Columbia.

(*continued on next page*)

(*continued*)

Study	Spatial coverage	Dataset	Data Period	Extreme metrics	Method	Key findings or significant trends (at P < 0.05)
					Trend slope and significance	
				number of days with snowfall		decreasing heavy snowfall trends over southern Canada; increase of about 2.2 days over the country's central and northern regions;
Yang et al. (2019)	Canada	Station data	1950–2012	ETCCDI indices	Theil–Sen estimator (Sen, 1968); Man-Kendal (Mann, 1945, Kendall, 1962)	significantly increasing trend in RX1day, RX5day, R95p, R99p, R10mm, CWD on average over Canada; significantly decreasing trend in CDD.
Choi et al. (2009)	Asia-Pacific Network Region (APN)	station data	1955–2007	ETCCDI indices	Least squares method and Kendall's τ–test	non-significant and spatially incoherent, stations showing increasing and decreasing trends are proportional,
Haylock et al. (2006)	South America	station data	1960–2000	ETCCDI indices	Kendall's Tau method (Kendall, 1938)	increasing RX1day, RX5day, R99p and R95p trends over southern Brazil and Paraguay; decreasing trends over the west coastal areas of Peru and southern Chile.

Study	Spatial coverage	Dataset	Data Period	Extreme metrics	Method	Key findings or significant trends (at $P <$ 0.05)
					Trend slope and significance	
de los Milagros Skansi et al. (2013)	South America	station data	1969–2009	ETCCDI indices	Kendall, 1955	trends are mostly non-significant;
Alexander and Arblaster (2017)	Australia	the Australian Water Availability Project (AWAP) dataset and HadEX2	1911–2010	ETCCDI indices	modified Ordinary Least Squares (OLS) (Hartmann et al., 2013)	extreme trends are generally non-significant, except SDII and CDD trends, which are significantly decreasing.

Appendix C. IPCC's reference regions (version 4) used in the 6th report for sub-continental analysis (Iturbide et al., 2020; IPCC, 2021). The map is produced with slight modification applied in ArcGIS using shape files provided by the Santander Meteorology Group ([10])

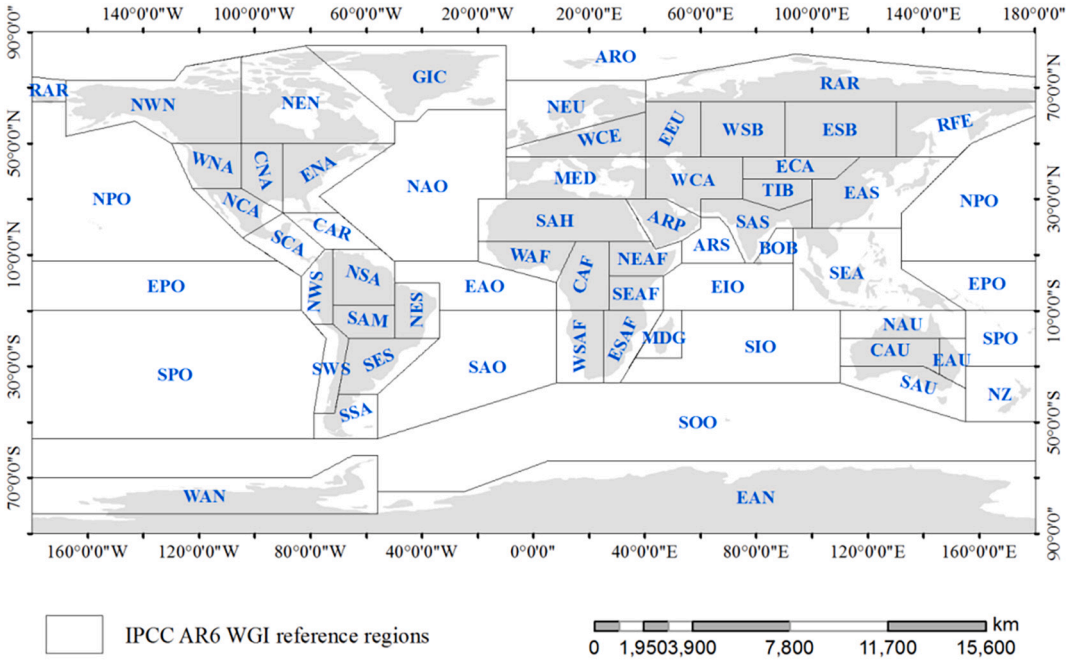

Appendix D. Evaluation of CHIRPS' precipitation estimates using selected stations from Ethiopia

We evaluate the daily precipitation estimates from CHIRPS V2.0 (Funk et al., 2015b) using *in situ* data from 14 selected stations in Ethiopia over the period 1995–2010. CHIRPS is a satellite-gauge hybrid product that provides precipitation estimates for the region between 50°S and 50°N, with spatial resolutions of 0.05° and 0.25°, and has been available since 1981 (Funk et al., 2015b). In this performance evaluation, the dataset with a spatial resolution of 0.05° is used. The daily precipitation data from the 14 Ethiopian stations are quality controlled and homogenized with an emphasis on

[10] https://github.com/SantanderMetGroup/ATLAS/tree/main/reference-regions

significant type-I change points (not shown here). We use the correlation coefficient, relative bias, and root mean square error (RMSE) to assess the accuracy of CHIRPS's estimates, and the probability of detection (POD), false alarm ratio (FAR), and equitable threat score (ETS) to evaluate CHIRPS's detection of precipitation occurrences (Ding et al., 2024; Xin et al., 2022). The POD assesses the ability to detect actual precipitation events, the FAR records false detections, and the ETS shows the proportion of accurate detections after accounting for random hits, thus reflecting the overall detection skill. The threshold for distinguishing between rainy and dry days is set at 1 mm of precipitation. Table D1 presents more details on the statistical metrics used for evaluation.

Table D1
Formulas, ranges and best values for the statistical metrics used in this assessment (Ding et al., 2024, Xin et al., 2022). S_i and O_i are daily precipitation series of CHIRPS and station (observed precipitation), respectively. H, F, M and H_e denote hits, false alarms, misses, and random hits, respectively.

Statistics	Formula	Range	Perfect Value
Probability of detection (POD)	$\frac{H}{H+M}$	0–1	1
False alarm ratio (FAR)	$\frac{F}{H+F}$	0–1	0
Equitable threat score (ETS)	$\frac{(H-H_e)}{(H+M+F-H_e)}; H_e = \frac{H+M)(H+F)}{(H+M+F+C)}$	−1/3–1	1
Correlation coefficient (Corr)	$\frac{\sum_{i=1}^{n}(S_i-O_i)}{\sum_{i=1}^{n}O_i}$	−1 - 1	1
Relative Bias	$\frac{\sum_{i=1}^{n}\lvert S_i-O_i\rvert}{\sum_{i=1}^{n}O_i}$	0 - $^{+}\infty$	0
Root mean square error (RMSE)	$\sqrt{\sum_{i=1}^{n}\frac{(S_i-O_i)^2}{n}}$	0 - $^{+}\infty$	0

Table D2 presents the results of the statistical scores. The statistical scores indicate a weak correlation between the daily precipitation estimates from CHIRPS V2.0 and the observations, with even lower values for stations located in southern Ethiopia, such as Arba Minch, Awassa, Jinka, and Konso. Similarly, Dinku et al. (2018) find low correlations between CHIRPS V2.0 and daily observations (2006−2014) using stations from northwest and southeast Ethiopia, with particularly lower correlations observed in the southeast. The product overestimates precipitation significantly over the southern stations, except for Hosana, while the relative bias scores over the remaining stations are good. The hybrid product generally exhibits lower POD and ETS scores, demonstrating weaker detection skills in this particular demonstration. As this is point-to-pixel comparisons, results may improve with pixel-to-pixel comparisons. Nonetheless, this demonstration supports the need for cautious use of precipitation products, especially in regions with sparse station networks and complex topographies. In such areas, the accuracy of precipitation estimates can vary significantly due to insufficient ground truth data and the challenges posed by complex terrains, compounded by uncertainties related to conversion algorithms.

Table D2
Statistical metrics results comparing daily precipitation estimates from CHIRPS V2.0 (Funk et al., 2015b) with *in situ* daily observations from 14 stations in Ethiopia for the period 1995–2010, using the grid cells containing the stations.

Station	POD	FAR	ETS	Cor	Relative bias	RMSE
Addis Ababa Obs	0.45	0.26	0.25	0.38	−0.05	8.69
Arba Minch	0.36	0.46	0.16	0.27	7.61	6.37
Awassa	0.41	0.41	0.17	0.27	7.07	6.28
Bahir Dar SYN	0.65	0.26	0.40	0.46	−0.08	9.39
Debre Berhan	0.37	0.34	0.21	0.35	0.16	9.16
Dire Dawa	0.51	0.46	0.26	0.41	−0.06	5.77
Hosana	0.41	0.29	0.22	0.33	0.00	8.85
Jimma	0.53	0.27	0.25	0.37	−0.03	8.88
Jinka	0.34	0.36	0.16	0.25	8.41	9.15
Konso	0.38	0.46	0.19	0.31	10.16	7.47
Mekele APO	0.42	0.40	0.26	0.47	0.16	6.24
Metehara (NMSA)	0.38	0.58	0.17	0.27	0.16	5.79
Robe	0.25	0.41	0.11	0.25	0.08	9.03
Wolkite	0.45	0.41	0.19	0.28	0.07	9.22

Data availability

Except the data from Ethiopian Meteorology Institute, all the data and materials associated with this review are from open sources, and their respective links and references are provided in the text.

References

Adeel, Z., Bakkensen, L., Cabrera-Rivera, O., Franco, E., Garfin, G.M., Mcpherson, R.A., Méndez, K., Wen, X., 2023. Challenges in and Opportunities for International Collaboration: Costing Flood Damages and Losses across Canada, Mexico, and the United States. Bull. Am. Meteorol. Soc. 104, E1323–E1332.

Afzali Gorooh, V., Hsu, K., Ferraro, R., Turk, J., Meng, H., Nguyen, P., Jimenez Arellano, C., Kalluri, S., Sorooshian, S., 2023. Advances in Precipitation Retrieval and Applications from Low-Earth-Orbiting Satellite Information. Bull. Am. Meteorol. Soc. 104, E1764–E1771.

Ageet, S., Fink, A.H., Maranan, M., Diem, J.E., Hartter, J., Ssali, A.L., Ayabagabo, P., 2022. Validation of satellite rainfall estimates over equatorial east Africa. J. Hydrometeorol. 23, 129–151.

Akinsanola, A.A., Ongoma, V., Kooperman, G.J., 2021. Evaluation of CMIP6 models in simulating the statistics of extreme precipitation over Eastern Africa. Atmos. Res. 254, 105509.

Alexander, L.V., 2016. Global observed long-term changes in temperature and precipitation extremes: A review of progress and limitations in Ipcc assessments and beyond. Weather Clim. Extremes 11, 4–16.

Alexander, L.V., Arblaster, J.M., 2017. Historical and projected trends in temperature and precipitation extremes in Australia in observations and CMIP5. Weather Clim.Extremes 15, 34–56.
Alexander, L., Herold, N., 2016. ClimPACT2: Indices and software. A document prepared on behalf of the Commission for Climatology (Ccl) Expert Team on Sector-specific Climate Indices (Et-Sci). Retrieved from. https://epic.awi.de/id/eprint/49274/1/ClimPACTv2_manual.pdf.
Alexander, L.V., Zhang, X., Peterson, T.C., Caesar, J., Gleason, B., Klein Tank, A., Haylock, M., Collins, D., Trewin, B., Rahimzadeh, F., 2006. Global observed changes in daily climate extremes of temperature and precipitation. J. Geophys. Res.-Atmos. 111.
Alexander, L.V., Hope, P., Collins, D., Trewin, B., Lynch, A., Nicholls, N., 2007. Trends in Australia's climate means and extremes: a global context. Aust. Meteorol. Mag. 56, 1–18.
Alexander, L.V., Fowler, H.J., Bador, M., Behrangi, A., Donat, M.G., Dunn, R., Funk, C., Goldie, J., Lewis, E., Rogé, M., 2019. On the use of indices to study extreme precipitation on sub-daily and daily timescales. Environ. Res. Lett. 14, 125008.
Alexander, L.V., Bador, M., Roca, R., Contractor, S., Donat, M.G., Nguyen, P.L., 2020. Intercomparison of annual precipitation indices and extremes over global land areas from in situ, space-based and reanalysis products. Environ. Res. Lett. 15, 055002.
Alizadeh, O., Babaei, M., 2022. Seasonally dependent precipitation changes and their driving mechanisms in Southwest Asia. Clim. Chang. 171, 20.
Almeida, C., Oliveira-Júnior, J., Delgado, R., Cubo, P., Ramos, M., 2017. Spatiotemporal rainfall and temperature trends throughout the Brazilian Legal Amazon, 1973–2013. Int. J. Climatol. 37, 2013–2026.
Al-Zu'bi, M., Dejene, S.W., Hounkpè, J., Kupika, O.L., Lwasa, S., Mbenge, M., Mwongera, C., Ouedraogo, N.S., Touré, N.D.E., 2022. African perspectives on climate change research. Nat. Clim. Chang. 12, 1078–1084.
Aravena, J.C., Luckman, B.H., 2009. Spatio-temporal rainfall patterns in southern South America. Inte. J. Climatol. J. R. Meteorol. Soc. 29, 2106–2120.
Bekele-Biratu, E., Thiaw, W.M., Korecha, D., 2018. Sub-seasonal variability of the Belg rains in Ethiopia.
Benestad, R.E., Parding, K.M., Erlandsen, H.B., Mezghani, A., 2019. A simple equation to study changes in rainfall statistics. Environ. Res. Lett. 14, 084017.
Bliefernicht, J., Salack, S., Waongo, M., Annor, T., Laux, P., Kunstmann, H., 2021. Towards a historical precipitation database for West Africa: Overview, quality control and harmonization. Int. J. Climatol. 42, 4001–4023.
Brönnimann, S., Brugnara, Y., Allan, R.J., Brunet, M., Compo, G.P., Crouthamel, R.I., Jones, P.D., Jourdain, S., Luterbacher, J., Siegmund, P., 2018. A roadmap to climate data rescue services. Geosci. Data J. 5, 28–39.
Brunet, M., Gilabert, A., Jones, P., Siegmund, P., 2020. Identifying Data Rescue gaps and issues.
Caloiero, T., Caloiero, P., Frustaci, F., 2018. Long-term precipitation trend analysis in Europe and in the Mediterranean basin. Water Environ. J. 32, 433–445.
Caporali, E., Lompi, M., Pacetti, T., Chiarello, V., Fatichi, S., 2021. A review of studies on observed precipitation trends in Italy. Int. J. Climatol. 41, E1–E25.
Carvalho, L.M., 2020. Assessing precipitation trends in the Americas with historical data: A review. Wiley Interdiscip. Rev. Clim. Chang. 11, e627.
Cavalcante, R.B.L., Da Silva Ferreira, D.B., Pontes, P.R.M., Tedeschi, R.G., Da Costa, C.P.W., De Souza, E.B., 2020. Evaluation of extreme rainfall indices from Chirps precipitation estimates over the Brazilian Amazonia. Atmos. Res. 238, 104879.
Chaney, N.W., Sheffield, J., Villarini, G., Wood, E.F., 2014. Development of a high-resolution gridded daily meteorological dataset over sub-Saharan Africa: Spatial analysis of trends in climate extremes. J. Clim. 27, 5815–5835.
Chang, M., Liu, B., Martinez-Villalobos, C., Ren, G., Li, S., Zhou, T., 2020. Changes in extreme precipitation accumulations during the warm season over continental China. J. Clim. 33, 10799–10811.
Chen, M., Shi, W., Xie, P., Silva, V.B., Kousky, V.E., Wayne Higgins, R., Janowiak, J.E., 2008. Assessing objective techniques for gauge-based analyses of global daily precipitation. J. Geophys. Res.-Atmos. 113.
Chen, C., Li, Z., Song, Y., Duan, Z., Mo, K., Wang, Z., Chen, Q., 2020. Performance of multiple satellite precipitation estimates over a typical arid mountainous area of China: Spatiotemporal patterns and extremes. J. Hydrometeorol. 21, 533–550.
Chen, H., Yong, B., Kirstetter, P.-E., Wang, L., Hong, Y., 2021. Global component analysis of errors in three satellite-only global precipitation estimates. Hydrol. Earth Syst. Sci. 25, 3087–3104.
Choi, G., Collins, D., Ren, G., Trewin, B., Baldi, M., Fukuda, Y., Afzaal, M., Pianmana, T., Gomboluudev, P., Huong, P.T.T., 2009. Changes in means and extreme events of temperature and precipitation in the Asia-Pacific Network region, 1955–2007. Inte. J. Climatol. J. R. Meteorol. Soc. 29, 1906–1925.
Coly, S.M., Zorom, M., Leye, B., Karambiri, H., Guiro, A., 2023. Learning from history of natural disasters in the Sahel: A comprehensive analysis and lessons for future resilience. Environ. Sci. Pollut. Res. 1–13.
Contractor, S., Donat, M.G., Alexander, L.V., 2018. Intensification of the daily wet day rainfall distribution across Australia. Geophys. Res. Lett. 45, 8568–8576.
Contractor, S., Donat, M.G., Alexander, L.V., Ziese, M., Meyer-Christoffer, A., Schneider, U., Rustemeier, E., Becker, A., Durre, I., Vose, R.S., 2020. Rainfall Estimates on a Gridded Network (Regen)–a global land-based gridded dataset of daily precipitation from 1950 to 2016. Hydrol. Earth Syst. Sci. 24, 919–943.
Contractor, S., Donat, M.G., Alexander, L.V., 2021. Changes in observed daily precipitation over global land areas since 1950. J. Clim. 34, 3–19.
Crétat, J., Vizy, E.K., Cook, K.H., 2014. How well are daily intense rainfall events captured by current climate models over Africa? Clim. Dyn. 42, 2691–2711.
Da Silva, P.E., Silva, Santos E., Spyrides, M.H.C., Andrade, L.D.M.B., 2019. Precipitation and air temperature extremes in the Amazon and northeast Brazil. Int. J. Climatol. 39, 579–595.
Dai, A., 2021. Hydroclimatic trends during 1950–2018 over global land. Clim. Dyn. 56, 4027–4049.
Danco, J.F., Deangelis, A.M., Raney, B.K., Broccoli, A.J., 2016. Effects of a warming climate on daily snowfall events in the Northern Hemisphere. J. Clim. 29, 6295–6318.
Davis, R.E., Lowit, M.B., Knappenberger, P.C., Legates, D.R., 1999. A climatology of snowfall-temperature relationships in Canada. J. Geophys. Res.-Atmos. 104, 11985–11994.
De Barros Soares, D., Lee, H., Loikith, P.C., Barkhordarian, A., Mechoso, C.R., 2017. Can significant trends be detected in surface air temperature and precipitation over South America in recent decades? Int. J. Climatol. 37, 1483–1493.
De Los Milagros Skansi, M., Brunet, M., Sigró, J., Aguilar, E., Groening, J.A.A., Bentancur, O.J., Geier, Y.R.C., Amaya, R.L.C., Jácome, H., Ramos, A.M., 2013. Warming and wetting signals emerging from analysis of changes in climate extreme indices over South America. Glob. Planet. Chang. 100, 295–307.
Deng, H., Pepin, N., Chen, Y., 2017. Changes of snowfall under warming in the Tibetan Plateau. J. Geophys. Res.-Atmos. 122, 7323–7341.
Dey, R., Lewis, S.C., Arblaster, J.M., Abram, N.J., 2019. A review of past and projected changes in Australia's rainfall. Wiley Interdiscip. Rev. Clim. Chang. 10, e577.
Dezfuli, A.K., Ichoku, C.M., Huffman, G.J., Mohr, K.I., Selker, J.S., Van De Giesen, N., Hochreutener, R., Annor, F.O., 2017. Validation of Imerg precipitation in Africa. J. Hydrometeorol. 18, 2817–2825.
Ding, Y., Wang, F., Lu, Z., Sun, P., Wei, R., Zhou, L., Ao, T., 2024. Assessments of various precipitation product performances and disaster monitoring utilities over the Tibetan Plateau. Sci. Rep. 14, 19740.
Dinku, T., 2019. Challenges with Availability and Quality of Climate Data in Africa. Extreme Hydrology and Climate Variability. Elsevier.
Dinku, T., Funk, C., Peterson, P., Maidment, R., Tadesse, T., Gadain, H., Ceccato, P., 2018. Validation of the Chirps satellite rainfall estimates over eastern Africa. Q. J. R. Meteorol. Soc. 144, 292–312.
Donat, M.G., Alexander, L.V., Yang, H., Durre, I., Vose, R., Caesar, J., 2013a. Global land-based datasets for monitoring climatic extremes. Bull. Am. Meteorol. Soc. 94, 997–1006.
Donat, M., Alexander, L.V., Yang, H., Durre, I., Vose, R., Dunn, R.J., Willett, K.M., Aguilar, E., Brunet, M., Caesar, J., 2013b. Updated analyses of temperature and precipitation extreme indices since the beginning of the twentieth century: The HadEX2 dataset. J. Geophys. Res.-Atmos. 118, 2098–2118.
Donat, M., Peterson, T., Brunet, M., King, A., Almazroui, M., Kolli, R., Boucherf, D., Al-Mulla, A.Y., Nour, A.Y., Aly, A.A., 2014. Changes in extreme temperature and precipitation in the Arab region: long-term trends and variability related to Enso and Nao. Int. J. Climatol. 34, 581–592.
Dosio, A., Pinto, I., Lennard, C., Sylla, M.B., Jack, C., Nikulin, G., 2021. What can we know about recent past precipitation over Africa? Daily characteristics of African precipitation from a large ensemble of observational products for model evaluation. Earth Space Sci. 8 e2020EA001466.
Duan, W., He, B., Takara, K., Luo, P., Hu, M., Alias, N.E., Nover, D., 2015. Changes of precipitation amounts and extremes over Japan between 1901 and 2012 and their connection to climate indices. Clim. Dyn. 45, 2273–2292.
Dufera, J.A., Yate, T.A., Kenea, T.T., 2023. Spatiotemporal analysis of drought in Oromia regional state of Ethiopia over the period 1989 to 2019. Nat. Hazards 1–41.
Dunn, R., Donat, M., Alexander, L., 2014. Investigating uncertainties in global gridded datasets of climate extremes. Clim. Past 10, 2171–2199.
Dunn, R.J., Alexander, L.V., Donat, M.G., Zhang, X., Bador, M., Herold, N., Lippmann, T., Allan, R., Aguilar, E., Barry, A.A., 2020. Development of an updated global land in situ-based data set of temperature and precipitation extremes: HadEX3. J. Geophys. Res.-Atmos. 125 e2019JD032263.
Easterling, D.R., Arnold, J., Knutson, T., Kunkel, K., Legrande, A., Leung, L.R., Vose, R., Waliser, D., Wehner, M., 2017. Precipitation change in the United States.
EPA, 2022. Climate Change Indicators: Weather and Climate [Online]. United States Environmental Protection Agency. Available: https://www.epa.gov/climate-indicators/weather-climate. Accessed January 29, 2024.
Feng, X., Liu, C., Xie, F., Lu, J., Chiu, L.S., Tintera, G., Chen, B., 2019. Precipitation characteristic changes due to global warming in a high-resolution (16 km) Ecmwf simulation. Q. J. R. Meteorol. Soc. 145, 303–317.
Funk, C., Nicholson, S.E., Landsfeld, M., Klotter, D., Peterson, P., Harrison, L., 2015a. The centennial trends greater horn of Africa precipitation dataset. Scientific data 2, 1–17.
Funk, C., Peterson, P., Landsfeld, M., Pedreros, D., Verdin, J., Shukla, S., Husak, G., Rowland, J., Harrison, L., Hoell, A., 2015b. The climate hazards infrared precipitation with stations—a new environmental record for monitoring extremes. Scientific data 2, 1–21.
Gebrechorkos, S.H., Hülsmann, S., Bernhofer, C., 2017. Evaluation of multiple climate data sources for managing environmental resources in East Africa. Hydrol. Earth Syst. Sci. 22, 4547–4564.
Gebrechorkos, S.H., Hülsmann, S., Bernhofer, C., 2018. Changes in Temperature and Precipitation Extremes in Ethiopia, Kenya, and Tanzania. Int. J. Climatol. 39, 18–30.
Giannini, A., Biasutti, M., Held, I.M., Sobel, A.H., 2008. A global perspective on African climate. Clim. Chang. 90, 359–383.
Gibba, P., Sylla, M.B., Okogbue, E.C., Gaye, A.T., Nikiema, M., Kebe, I., 2019. State-of-the-art climate modeling of extreme precipitation over Africa: analysis of Cordex added-value over CMIP5. Theor. Appl. Climatol. 137, 1041–1057.
Giorgi, F., Raffaele, F., Coppola, E., 2019. The response of precipitation characteristics to global warming from climate projections. Earth System Dynam. 10, 73–89.
Hadi, S.J., Tombul, M., 2018. Long-term spatiotemporal trend analysis of precipitation and temperature over Turkey. Meteorol. Appl. 25, 445–455.

Haghtalab, N., Moore, N., Heerspink, B.P., Hyndman, D.W., 2020. Evaluating spatial patterns in precipitation trends across the Amazon basin driven by land cover and global scale forcings. Theor. Appl. Climatol. 140, 411–427.
Haile, G.G., Tang, Q., Sun, S., Huang, Z., Zhang, X., Liu, X., 2019. Droughts in East Africa: Causes, impacts and resilience. Earth Sci. Rev. 193, 146–161.
Hamed, K.H., Rao, A.R., 1998. A modified Mann-Kendall trend test for autocorrelated data. J. Hydrol. 204, 182–196.
Han, H., Abitew, T.A., Park, S., Green, C.H., Jeong, J., 2023. Spatiotemporal Evaluation of Satellite-Based Precipitation Products in the Colorado River Basin. J. Hydrometeorol. 24, 1739–1754.
Harp, R.D., Horton, D.E., 2022. Observed changes in daily precipitation intensity in the United States. Geophys. Res. Lett. 49 e2022GL099955.
Harris, I., Jones, P.D., Osborn, T.J., Lister, D.H., 2014. Updated high-resolution grids of monthly climatic observations–the Cru TS3. 10 Dataset. Int. J. Climatol. 34, 623–642.
Harris, I., Osborn, T.J., Jones, P., Lister, D., 2020. Version 4 of the Cru Ts monthly high-resolution gridded multivariate climate dataset. Scientific data 7, 109.
Harrison, L., Funk, C., Peterson, P., 2019. Identifying changing precipitation extremes in Sub-Saharan Africa with gauge and satellite products. Environ. Res. Lett. 14, 085007.
Hartmann, D.L., Tank, A.M.K., Rusticucci, M., Alexander, L.V., Brönnimann, S., Charabi, Y.A.R., Dentener, F.J., Dlugokencky, E.J., Easterling, D.R., Kaplan, A., 2013. Observations: atmosphere and surface. *Climate change 2013 the physical science basis: Working group I contribution to the fifth assessment report of the intergovernmental panel on climate change*. Cambridge University Press.
Haylock, M.R., Peterson, T.C., Alves, L.M., Ambrizzi, T., Anunciação, Y., Báez, J., Barros, V., Berlato, M., Bidegain, M., Coronel, G., 2006. Trends in total and extreme South American rainfall in 1960–2000 and links with sea surface temperature. J. Clim. 19, 1490–1512.
He, J., Feng, P., Wang, B., Zhuang, W., Zhang, Y., Liu, D.L., Cleverly, J., Huete, A., Yu, Q., 2022. Centennial annual rainfall pattern changes show an increasing trend with higher variation over Northern Australia. J. Hydrometeorol. 23, 1333–1349.
Herold, N., Behrangi, A., Alexander, L.V., 2017. Large uncertainties in observed daily precipitation extremes over land. J. Geophys. Res.-Atmos. 122, 668–681.
Hoell, A., Gaughan, A.E., Magadzire, T., Harrison, L., 2021. The Modulation of Daily Southern Africa Precipitation by El Niño–Southern Oscillation across the Summertime Wet Season. J. Clim. 34, 1115–1134.
Hoerling, M., Eischeid, J., Perlwitz, J., Quan, X.-W., Wolter, K., Cheng, L., 2016. Characterizing recent trends in Us heavy precipitation. J. Clim. 29, 2313–2332.
Hu, Z., Zhou, Q., Chen, X., Qian, C., Wang, S., Li, J., 2017. Variations and changes of annual precipitation in Central Asia over the last century. Int. J. Climatol. 37, 157–170.
Hulme, M., Doherty, R., Ngara, T., New, M., Lister, D., 2001. African climate change: 1900-2100. Clim. Res. 17, 145–168.
IPCC, 2021. In: Masson-Delmotte, V., Zhai, P., Pirani, A., Connors, S.L., Péan, C., Berger, S., Caud, N., Chen, Y., Goldfarb, L., Gomis, M.I., Huang, M., Leitzell, K., Lonnoy, E., Matthews, J.B.R., Maycock, T.K., Waterfield, T., Yelekçi, O., Yu, R., Zhou, B. (Eds.), Climate Change 2021: The Physical Science Basis. Contribution of Working Group I to the Sixth Assessment Report of the Intergovernmental Panel on Climate Change.
IPCC, 2022. In: Pörtner, H.O., Tignor, M., Poloczanska, E.S., Mintenbeck, K., Alegría, A., Craig, M., Langsdorf, S., Löschke, S., Möller, V., Okem, A., Rama, B. (Eds.), Climate Change 2022: Impacts, Adaptation, and Vulnerability. Contribution of Working Group Ii to the Sixth Assessment Report of the Intergovernmental Panel on Climate Change.
Iturbide, M., Gutiérrez, J.M., Alves, L.M., Bedia, J., Cerezo-Mota, R., Cimadevilla, E., Cofiño, A.S., Di Luca, A., Faria, S.H., Gorodetskaya, I.V., 2020. An update of Ipcc climate reference regions for subcontinental analysis of climate model data: definition and aggregated datasets. Earth Syst. Scie. Data 12, 2959–2970.
Kagone, S., Velpuri, N.M., Khand, K., Senay, G.B., Van Der Valk, M.R., Goode, D.J., Hantash, S.A., Al-Momani, T.M., Momejian, N., Eggleston, J.R., 2023. Satellite precipitation bias estimation and correction using in situ observations and climatology isohyets for the Mena region. J. Arid Environ. 215, 105010.
Karl, T.R., Knight, R.W., 1998. Secular trends of precipitation amount, frequency, and intensity in the United States. Bull. Am. Meteorol. Soc. 79, 231–242.
Kaspar, F., Andersson, A., Ziese, M., Hollmann, R., 2022. Contributions to the improvement of climate data availability and quality for sub-Saharan Africa. Front. Clim. 3, 815043.
Kendall, M.G., 1938. A new measure of rank correlation. Biometrika 30, 81–93.
Kendall, M.G., 1955. Further contributions to the theory of paired comparisons. Biometrics 11, 43–62.
Kendall, M., 1962. Rank Correlation Methods. Hafner Pub. *Co.*, New York, Ny, Usa, p. 199.
Kidd, C., Becker, A., Huffman, G.J., Muller, C.L., Joe, P., Skofronick-Jackson, G., Kirschbaum, D.B., 2017. So, how much of the Earth's surface is covered by rain gauges? Bull. Am. Meteorol. Soc. 98, 69–78.
Kruger, A.C., Nxumalo, M., 2017. Historical rainfall trends in South Africa: 1921–2015. Water SA 43, 285–297.
Kumar, V., Jain, S.K., Singh, Y., 2010. Analysis of long-term rainfall trends in India. Hydrol. Scie. J. 55, 484–496.
Kuttippurath, J., Murasingh, S., Stott, P., Sarojini, B.B., Jha, M.K., Kumar, P., Nair, P., Varikoden, H., Raj, S., Francis, P., 2021. Observed rainfall changes in the past century (1901–2019) over the wettest place on Earth. Environ. Res. Lett. 16, 024018.
Le Coz, C., Van De Giesen, N., 2020. Comparison of rainfall products over sub-saharan africa. J. Hydrometeorol. 21, 553–596.
Lewis, E., Guerreiro, S., Blenkinsop, S., Fowler, H.J., 2019. Quality Control of a Global Sub-daily Precipitation Dataset and Derived Extreme Precipitation Indices. Geophys. Res. 21, EGU2019–16634.
Li, J., Yu, R., 2014. A method to linearly evaluate rainfall frequency–intensity distribution. J. Appl. Meteorol. Climatol. 53, 928–934.
Lieber, M., Chin-Hong, P., Kelly, K., Dandu, M., Weiser, S.D., 2022. A systematic review and meta-analysis assessing the impact of droughts, flooding, and climate variability on malnutrition. Global Public Health 17, 68–82.
Liebmann, B., Hoerling, M.P., Funk, C., Bladé, I., Dole, R.M., Allured, D., Quan, X., Pegion, P., Eischeid, J.K., 2014. Understanding recent eastern Horn of Africa rainfall variability and change. J. Clim. 27, 8630–8645.
Lim Kam Sian, K.T.C., Wang, J., Ayugi, B.O., Nooni, I.K., Ongoma, V., 2021. Multi-decadal variability and future changes in precipitation over Southern Africa. Atmosphere 12, 742.
Liu, J., Wu, D., Li, Y., Ren, H., Zhao, Y., Sun, X., Zhang, H., Ji, M., 2022. Spatiotemporal variation of precipitation on a global scale from 1960 to 2016 in a new normalized daily precipitation dataset. Int. J. Climatol. 42, 3648–3665.
López-Bermeo, C., Montoya, R.D., Caro-Lopera, F.J., Díaz-García, J.A., 2022. Validation of the accuracy of the Chirps precipitation dataset at representing climate variability in a tropical mountainous region of South America. Phys. Chem. Earth Parts A/B/C 127, 103184.
Lüdecke, H.-J., Müller-Plath, G., Wallace, M.G., Lüning, S., 2021. Decadal and multidecadal natural variability of African rainfall. J. Hydrol. Reg. Studi. 34, 100795.
Macharia, D., Fankhauser, K., Selker, J.S., Neff, J.C., Thomas, E.A., 2022. Validation and intercomparison of satellite-based rainfall products over Africa with Tahmo in situ rainfall observations. J. Hydrometeorol. 23, 1131–1154.
Madakumbura, G.D., Thackeray, C.W., Norris, J., Goldenson, N., Hall, A., 2021. Anthropogenic influence on extreme precipitation over global land areas seen in multiple observational datasets. Nat. Commun. 12, 3944.
Maggioni, V., Meyers, P.C., Robinson, M.D., 2016. A review of merged high-resolution satellite precipitation product accuracy during the Tropical Rainfall Measuring Mission (Trmm) era. J. Hydrometeorol. 17, 1101–1117.
Maidment, R.I., Allan, R.P., Black, E., 2015. Recent observed and simulated changes in precipitation over Africa. Geophys. Res. Lett. 42, 8155–8164.
Mann, H.B., 1945. Nonparametric tests against trend. Econometrica J. Econo. Soci. 245–259.
Matsuura, K., Willmott, C.J., 2018. Terrestrial precipitation: 1900–2017 gridded monthly time series. Department of Geography, University of Delaware, Newark, De, Electronic, p. 19716.
Mcbride, C.M., Kruger, A.C., Dyson, L., 2022. Changes in extreme daily rainfall characteristics in South Africa: 1921–2020. Weather Clim. Extremes 38, 100517.
Mckay, R.C., Boschat, G., Rudeva, I., Pepler, A., Purich, A., Dowdy, A., Hope, P., Gillett, Z.E., Rauniyar, S., 2023. Can southern Australian rainfall decline be explained? A review of possible drivers. Wiley Interdiscip. Rev. Clim. Chang. 14, e820.
Mekonnen, K., Velpuri, N.M., Leh, M., Akpoti, K., Owusu, A., Tinonetsana, P., Hamouda, T., Ghansah, B., Paranamana, T.P., Munzimi, Y., 2023. Accuracy of satellite and reanalysis rainfall estimates over Africa: A multi-scale assessment of eight products for continental applications. J. Hydrol. Reg. Studi. 49, 101514.
Mena, M.M., Kenea, T.T., Yate, T.A., 2023. Spatial patterns and temporal dynamics of drought in southern Ethiopia from 1981 to 2100. Int. J. Climatol. 43, 7234–7255.
Menne, M.J., Durre, I., Vose, R.S., Gleason, B.E., Houston, T.G., 2012. An overview of the global historical climatology network-daily database. J. Atmos. Ocean. Technol. 29, 897–910.
Menne, M.J., Williams Jr., C., Vose, R.S., 2015. United States historical climatology network daily temperature, precipitation, and snow data. Carbon Dioxide Information Analysis Center, Oak Ridge National Laboratory, Oak Ridge, Tennessee.
Merz, B., Blöschl, G., Vorogushyn, S., Dottori, F., Aerts, J.C., Bates, P., Bertola, M., Kemter, M., Kreibich, H., Lall, U., 2021. Causes, impacts and patterns of disastrous river floods. Nat. Rev. Earth Environ. 2, 592–609.
Monadjem, A., 2023. African Ark: Mammals, Landscape and the Ecology of a Continent. Nyu Press.
Mondal, A., Khare, D., Kundu, S., 2015. Spatial and temporal analysis of rainfall and temperature trend of India. Theor. Appl. Climatol. 122, 143–158.
Moustakis, Y., Onof, C.J., Paschalis, A., 2020. Atmospheric convection, dynamics and topography shape the scaling pattern of hourly rainfall extremes with temperature globally. Commun. Earth Environ. 1, 11.
Muthoni, F.K., Odongo, V.O., Ochieng, J., Mugalavai, E.M., Mourice, S.K., Hoesche-Zeledon, I., Mwila, M., Bekunda, M., 2019. Long-term spatial-temporal trends and variability of rainfall over Eastern and Southern Africa. Theor. Appl. Climatol. 137, 1869–1882.
Myhre, G., Alterskjær, K., Stjern, C.W., Hodnebrog, Ø., Marelle, L., Samset, B.H., Sillmann, J., Schaller, N., Fischer, E., Schulz, M., 2019. Frequency of extreme precipitation increases extensively with event rareness under global warming. Sci. Rep. 9, 16063.
Nguyen, P., Thorstensen, A., Sorooshian, S., Hsu, K., Aghakouchak, A., Ashouri, H., Tran, H., Braithwaite, D., 2018. Global precipitation trends across spatial scales using satellite observations. Bull. Am. Meteorol. Soc. 99, 689–697.
Nicholson, S.E., 2019. A review of climate dynamics and climate variability in Eastern Africa. In: Limnology, Climatology and Paleoclimatology of the East African Lakes, pp. 25–56.
Nicholson, S.E., Funk, C., Fink, A.H., 2018. Rainfall over the African continent from the 19th through the 21st century. Glob. Planet. Chang. 165, 114–127.
Nicola, L., Notz, D., Winkelmann, R., 2023. Revisiting temperature sensitivity: how does Antarctic precipitation change with temperature? Cryosphere 17, 2563–2583.

Novella, N.S., Thiaw, W.M., 2013. African rainfall climatology version 2 for famine early warning systems. J. Appl. Meteorol. Climatol. 52, 588–606.
O'gorman, P.A., 2014. Contrasting responses of mean and extreme snowfall to climate change. Nature 512, 416–418.
O'gorman, P.A., 2015. Precipitation extremes under climate change. Curr. Clim. Chang. Rep. 1, 49–59.
Ombadi, M., Nguyen, P., Sorooshian, S., Hsu, K.-L., 2021. How much information on precipitation is contained in satellite infrared imagery? Atmos. Res. 256, 105578.
Omondi, P., Awange, J.L., Ogallo, L., Okoola, R., Forootan, E., 2012. Decadal rainfall variability modes in observed rainfall records over East Africa and their relations to historical sea surface temperature changes. J. Hydrol. 464, 140–156.
Omondi, P., Ogallo, L.A., Anyah, R., Muthama, J., Ininda, J., 2013. Linkages between global sea surface temperatures and decadal rainfall variability over Eastern Africa region. Int. J. Climatol. 33, 2082–2104.
Omondi, P.A.O., Awange, J.L., Forootan, E., Ogallo, L.A., Barakiza, R., Girmaw, G.B., Fesseha, I., Kululetera, V., Kilembe, C., Mbati, M.M., 2014. Changes in temperature and precipitation extremes over the Greater Horn of Africa region from 1961 to 2010. Int. J. Climatol. 34, 1262–1277.
Onyutha, C., 2016. Identification of sub-trends from hydro-meteorological series. Stoch. Env. Res. Risk A. 30, 189–205.
Onyutha, C., 2018. Trends and variability in African long-term precipitation. Stoch. Env. Res. Risk A. 32, 2721–2739.
Onyutha, C., 2020. Analyses of rainfall extremes in East Africa based on observations from rain gauges and climate change simulations by Cordex RCMs. Clim. Dyn. 54, 4841–4864.
Palmer, P.I., Wainwright, C.M., Dong, B., Maidment, R.I., Wheeler, K.G., Gedney, N., Hickman, J.E., Madani, N., Folwell, S.S., Abdo, G., 2023. Drivers and impacts of Eastern African rainfall variability. Nat. Rev. Earth Environ. 4, 254–270.
Papalexiou, S.M., Montanari, A., 2019. Global and regional increase of precipitation extremes under global warming. Water Resour. Res. 55, 4901–4914.
Parker, D., Good, E., Chadwick, R., 2011. Reviews of observational data available over Africa for monitoring, attribution and forecast evaluation. Met Office.
Peña-Angulo, D., Vicente-Serrano, S.M., Domínguez-Castro, F., Murphy, C., Reig, F., Tramblay, Y., Trigo, R., Luna, M., Turco, M., Noguera, I., 2020. Long-term precipitation in Southwestern Europe reveals no clear trend attributable to anthropogenic forcing. Environ. Res. Lett. 15, 094070.
Philandras, C., Nastos, P., Kapsomenakis, J., Douvis, K., Tselioudis, G., Zerefos, C., 2011. Long term precipitation trends and variability within the Mediterranean region. Nat. Hazards Earth Syst. Sci. 11, 3235–3250.
Powell, E.J., Keim, B.D., 2015. Trends in daily temperature and precipitation extremes for the southeastern United States: 1948–2012. J. Clim. 28, 1592–1612.
Ren, G., Zhou, Y., 2014. Urbanization effect on trends of extreme temperature indices of national stations over mainland China, 1961–2008. J. Clim. 27, 2340–2360.
Ren, G., Ren, Y., Yunjian, Z., Xiubao, S., Yanju, L., Yu, C., Tao, W., 2015. Spatial and temporal patterns of precipitation variability over mainland China: Ii: Recent trends. 水科学进展 26, 451–465.
Ren, G., Yuan, Y., Liu, Y., Ren, Y., Wang, T., Ren, X., 2016. Changes in precipitation over Northwest China. Arid Zone Res. 33, 1–19.
Ren, Y.-Y., Ren, G.-Y., Sun, X.-B., Shrestha, A.B., You, Q.-L., Zhan, Y.-J., Rajbhandari, R., Zhang, P.-F., Wen, K.-M., 2017. Observed changes in surface air temperature and precipitation in the Hindu Kush Himalayan region over the last 100-plus years. Adv. Clim. Chang. Res. 8, 148–156.
Ren, G., Chan, J.C., Kubota, H., Zhang, Z., Li, J., Zhang, Y., Zhang, Y., Yang, Y., Ren, Y., Sun, X., 2021. Historical and recent change in extreme climate over East Asia. Clim. Chang. 168, 1–19.
Ren, G., Zhan, Y., Ren, Y., Wen, K., Zhang, Y., Sun, X., Zhang, P., Zheng, X., Qin, Y., Zhang, S., 2023. Observed changes in temperature and precipitation over Asia, 1901-2020. Clim. Res. 90, 31–43.
Schär, C., Ban, N., Fischer, E.M., Rajczak, J., Schmidli, J., Frei, C., Giorgi, F., Karl, T.R., Kendon, E.J., Tank, A.M.K., 2016. Percentile indices for assessing changes in heavy precipitation events. Clim. Chang. 137, 201–216.
Schneider, U., Finger, P., Rustemeier, E., Ziese, M., Hänsel, S., 2022a. Global precipitation analysis products of the GPCC [Online]. Available: https://opendata.dwd.de/climate_environment/Gpcc/Pdf/Gpcc_intro_products_v2022.pdf. Accessed January 7 2024.
Schneider, U., Hänsel, S., Finger, P., Rustemeier, E., Ziese, M., 2022b. Gpcc Full Data Monthly Product Version 2022 (at 0.25°, 0.5°, 1.0°, 2.5°): Monthly Land-Surface Precipitation from Rain-Gauges built on Gts-based and Historical Data. Global Precipitation Climatology Centre.
Sen, P.K., 1968. Estimates of the regression coefficient based on Kendall's tau. J. Am. Stat. Assoc. 63, 1379–1389.
Stampoulis, D., Anagnostou, E.N., Nikolopoulos, E.I., 2013. Assessment of high-resolution satellite-based rainfall estimates over the Mediterranean during heavy precipitation events. J. Hydrometeorol. 14, 1500–1514.
Sugg, M., Runkle, J., Leeper, R., Bagli, H., Golden, A., Handwerger, L.H., Magee, T., Moreno, C., Reed-Kelly, R., Taylor, M., 2020. A scoping review of drought impacts on health and society in North America. Clim. Chang. 162, 1177–1195.
Sun, Q., Miao, C., Duan, Q., Ashouri, H., Sorooshian, S., Hsu, K.L., 2017. A review of global precipitation data sets: Data sources, estimation, and intercomparisons. Rev. Geophys. 56, 79–107.
Sun, Q., Zhang, X., Zwiers, F., Westra, S., Alexander, L.V., 2021. A global, continental, and regional analysis of changes in extreme precipitation. J. Clim. 34, 243–258.
Suriano, Z.J., Loewy, C., Uz, J., 2023. Synoptic Climatology of Central Us Snowfall. J. Appl. Meteorol. Climatol. 62, 1731–1743.
Teshome, A., Zhang, J., Demissie, T., Ma, Q., 2022. Observed and future spatiotemporal changes of rainfall extreme characteristics and their dynamic driver in June-August season over Africa. Atmos. Clim. Scie. 12, 358–382.
Tierney, J.E., Ummenhofer, C.C., Demenocal, P.B., 2015. Past and future rainfall in the Horn of Africa. Sci. Adv. 1, e1500682.
Tolhurst, G., Hope, P., Osburn, L., Rauniyar, S., 2023. Approaches to Understanding Decadal and Long-Term Shifts in Observed Precipitation Distributions in Victoria, Australia. J. Appl. Meteorol. Climatol. 62, 3–19.
Van Den Besselaar, E., Klein Tank, A., Buishand, T., 2013. Trends in European precipitation extremes over 1951–2010. Int. J. Climatol. 33, 2682–2689.
Varuolo-Clarke, A.M., Smerdon, J.E., Williams, A.P., Seager, R., 2021. Gross discrepancies between observed and simulated twentieth-to-twenty-first-century precipitation trends in southeastern South America. J. Clim. 34, 6441–6457.
Vicente-Serrano, S.M., Domínguez-Castro, F., Murphy, C., Hannaford, J., Reig, F., Peña-Angulo, D., Tramblay, Y., Trigo, R.M., Mac Donald, N., Luna, M.Y., 2020. Long-term variability and trends in meteorological droughts in Western Europe (1851–2018). Int. J. Climatol. 41, E690–E717.
Vincent, L., Zhang, X., Mekis, É., Wan, H., Bush, E., 2018. Changes in Canada's climate: Trends in indices based on daily temperature and precipitation data. Atmosphere-Ocean 56, 332–349.
Wang, X.L., Feng, Y., 2013. RHtests_dlyPrcp user manual. Climate Research Division, Atmospheric Science and Technology Directorate, Science and Technology Branch, Environment Canada: Toronto, On, Canada, 25, p. 2014.
Wang, X.L., Feng, Y., Cheng, V.Y., Xu, H., 2023. Observed precipitation trends inferred from Canada's homogenized monthly precipitation dataset. J. Clim. 36, 7957–7971.
WMO, 2008. Guide to meteorological instruments and methods of observation. WMO-NO. 8.
WMO, 2009. Guidelines on analysis of extremes in a changing climate in support of informed decisions for adaptation [Online]. [Accessed].
Wu, J., Gao, X.-J., 2013. A gridded daily observation dataset over China region and comparison with the other datasets. Chin. J. Geophys. 56, 1102–1111.
Wubaye, G.B., Gashaw, T., Worqlul, A.W., Dile, Y.T., Taye, M.T., Haileslassie, A., Zaitchik, B., Birhan, D.A., Adgo, E., Mohammed, J.A., 2023. Trends in rainfall and temperature extremes in Ethiopia: Station and agro-ecological zone levels of analysis. Atmosphere 14, 483.
Xiao-Juan, W., Tuo, Y., Xiao-Fan, L., Guo-Lin, F., 2023. Features of the New Climate Normal 1991–2020 and Possible Influences on Climate Monitoring and Prediction in China. Adv. Clim. Chang. Res. 14, 930–940.
Xie, P., Chen, M., Shi, W., 2010. Cpc unified gauge-based analysis of global daily precipitation. Preprints. In: 24th Conf. on Hydrology, Atlanta, Ga, Amer. Meteor. Soc.
Xin, Y., Yang, Y., Chen, X., Yue, X., Liu, Y., Yin, C., 2022. Evaluation of Imerg and ERA5 precipitation products over the Mongolian Plateau. Sci. Rep. 12, 21776.
Yang, S., Xu, W., Xu, Y., Li, Q., 2016. Development of a global historic monthly mean precipitation dataset. J. Meteorol. Res. 30, 217–231.
Yang, Y., Gan, T.Y., Tan, X., 2019. Spatiotemporal changes in precipitation extremes over Canada and their teleconnections to large-scale climate patterns. J. Hydrometeorol. 20, 275–296.
Yu, X., Gu, X., Kong, D., Zhang, Q., Cao, Q., Slater, L.J., Ren, G., Luo, M., Li, J., Liu, J., 2022. Asymmetrical shift toward less light and more heavy precipitation in an urban agglomeration of East China: Intensification by urbanization. Geophys. Res. Lett. 49 e2021GL097046.
Yue, S., Pilon, P., Cavadias, G., 2002. Power of the Mann–Kendall and Spearman's rho tests for detecting monotonic trends in hydrological series. J. Hydrol. 259, 254–271.
Zeder, J., Fischer, E.M., 2020. Observed extreme precipitation trends and scaling in Central Europe. Weather Clim. Extremes 29, 100266.
Zhai, P., Zhang, X., Wan, H., Pan, X., 2005. Trends in total precipitation and frequency of daily precipitation extremes over China. J. Clim. 18, 1096–1108.
Zhan, Y., Ren, G., 2023. Change in mean and extreme precipitation in eastern China since 1901. Clim. Res. 91, 1–19.
Zhan, Y.-J., Ren, G.-Y., Shrestha, A.B., Rajbhandari, R., Ren, Y.-Y., Sanjay, J., Xu, Y., Sun, X.-B., You, Q.-L., Wang, S., 2017. Changes in extreme precipitation events over the Hindu Kush Himalayan region during 1961–2012. Adv. Clim. Chang. Res. 8, 166–175.
Zhan, Y., Ren, G., Yang, S., 2018. Change in precipitation over the Asian continent from 1901-2016 based on a new multi-source dataset. Clim. Res. 76, 41–57.
Zhan, Y., Ren, G., Wang, P., 2019. The influence of data processing on constructing regional average precipitation time series. Adv. Clim. Chang. Res. 15, 584.
Zhan, Y., Chen, D., Liao, J., Ju, X.H., Zhao, Y.F., Ren, G., 2022. Construction of a daily precipitation dataset of 60 city stations in China for the period 1901-2019. Adv. Clim. Chang. Res. 18, 670.
Zhang, X., Yang, F., 2004. RClimDex (1.0) user manual. Clim. Res. Branch Environ. Can. 22, 13–14.
Zhang, W., Zhou, T., 2019. Significant increases in extreme precipitation and the associations with global warming over the global land monsoon regions. J. Clim. 32, 8465–8488.
Zhang, X., Vincent, L.A., Hogg, W., Niitsoo, A., 2000. Temperature and precipitation trends in Canada during the 20th century. Atmosphere-ocean 38, 395–429.
Zhang, X., Alexander, L., Hegerl, G.C., Jones, P., Tank, A.K., Peterson, T.C., Trewin, B., Zwiers, F.W., 2011. Indices for monitoring changes in extremes based on daily temperature and precipitation data. Wiley Interdiscip. Rev. Clim. Chang. 2, 851–870.
Zhang, Y., Ren, Y., Ren, G., Wang, G., 2019. Bias correction of gauge data and its effect on precipitation climatology over mainland China. J. Appl. Meteorol. Climatol. 58, 2177–2196.

Zhang, Y., Ren, Y., Ren, G., Wang, G., 2020. Precipitation trends over mainland China from 1961–2016 after removal of measurement biases. J. Geophys. Res.-Atmos. 125 e2019JD031728.
Zhang, Y., Wu, C., Yeh, P.J.-F., Li, J., Hu, B.X., Feng, P., Jun, C., 2022. Evaluation and comparison of precipitation estimates and hydrologic utility of Chirps, Trmm 3B42 V7 and Persiann-Cdr products in various climate regimes. Atmos. Res. 265, 105881.
Zhou, B., Xu, Y., Wu, J., Dong, S., Shi, Y., 2016. Changes in temperature and precipitation extreme indices over China: Analysis of a high-resolution grid dataset. Int. J. Climatol. 36, 1051–1066.
Zhou, B., Wang, Z., Shi, Y., Xu, Y., Han, Z., 2018. Historical and future changes of snowfall events in China under a warming background. J. Clim. 31, 5873–5889.
Ziese, M., Rauthe-Schöch, A., Becker, A., Finger, P., Rustemeier, E., Schneider, U., 2020. GPCC Full Data Daily Version 2020 at 1.0°: Daily land-surface precipitation from rain-gauges built on GTS-based and historic data.
Ziese, M., Rauthe-Schöch, A., Becker, A., Finger, P., Rustemeier, E., Schneider, U., 2022. GPCC Full Data Daily Version 2022 at 1.0°: daily land-surface precipitation from rain-gauges built on GTS-based and historic data.
Zittis, G., 2018. Observed rainfall trends and precipitation uncertainty in the vicinity of the Mediterranean, Middle East and North Africa. Theor. Appl. Climatol. 134, 1207–1230.